A Computational Framework for Assessing Mission Outcomes with Humans and Robots

Xiaoyu Liu,[*] Amir Behjat,[†] Shirley J. Dyke,[‡] Dawn Whitaker,[§] Julio Ramirez,[¶] and Ilias Bilionis.[**]
Purdue University, West Lafayette, IN 47907, USA

Space exploration is progressing toward long-term missions that will involve both human and robotic agents in operations in lunar space habitats, the Gateway space station, and Moon-to-Mars program. These missions require high-level intelligence and sustained performance over extended periods. Analyzing agent performance solely on a task level is insufficient for such complex applications because the resources consumed by agents are coupled with the utility they provide under various conditions. Additionally, factors like the agents' availability to respond to hazard events—impacted by factors including human sleep cycles and robot charging times—must be considered. Understanding how resources, utility, and availability interrelate is crucial for early-phase decision-making, assessing logistics, and for steering investments in promising directions. In this paper, we use the rapid simulation capabilities of the Control-oriented Dynamic Computational Modeling (CDCM) to explore the trade space involving a human agent (HA) and a robotic agent (RA) tasked with maintaining a smart space habitat (SSH). Our approach models two independent parallel scenarios as systems of systems using stochastic methods to account for mission variabilities. A human scientist (HS) is included to quantify the mission's research outcomes. The outcomes generated by the HS serve as the metric to compare the agents' performance, alongside the costs associated with engaging the HA and RA.

[*] Postdoctoral Researcher, School of Mechanical Engineering, Purdue University, liu1787@purdue.edu.
[†] Postdoctoral Researcher, School of Mechanical Engineering, Purdue University, abehjat@purdue.edu.
[‡] Professor, School of Mechanical Engineering, Purdue University, AIAA Member, sdyke@purdue.edu.
[§] Associate Director, Indiana Space Grant Consortium, dwhitaker@purdue.edu.
[¶] Professor, Lyles School of Civil Engineering, Purdue University, ramirez@purdue.edu.
[**] Associate Professor, School of Mechanical Engineering, Purdue University, ibilion@purdue.edu.

Nomenclature

CDCM = Control-Oriented Dynamic Computational Modeling Framework

HA = Human Agent

HMS = Health management system

HS = Human Scientist

IE = Interior Environment Model

M-ESM = Modified Version of Equivalent System Mass

MS = Micrometeorite Strike

PG = Power Generation System

RA = Robotic Agent

SRH = Science Research Hours

SSH = Smart Space Habitat

ST = Structural System

SoS = System of Systems

I. Introduction

Human space flight missions have achieved remarkable milestones over the past six decades, showcasing the extraordinary capabilities of humans in space exploration. Beginning with Yuri Gagarin's historic flight in 1961 as the first human in space [1], followed by the Apollo missions that successfully landed astronauts on the Moon and returned them safely to Earth [2], humanity has continually pushed the boundaries of what is possible. The Space Shuttle program enabled extended missions in low Earth orbit, and facilitated the deployment and repair of satellites like the Hubble Space Telescope [3]. Furthermore, the International Space Station, a collaborative effort involving multiple countries, has served as a microgravity laboratory for over two decades, where astronauts have conducted thousands of experiments in biology, physics, astronomy, Earth science, and more [4–7]. These achievements have not only advanced scientific knowledge but have also demonstrated human adaptability, problem-solving skills, and the ability to perform complex tasks in the challenging environment of space.

Despite these successes, human spaceflight faces significant challenges that necessitate the integration of greater automation, robotics, and autonomy[8–11]. In space, astronauts are exposed to harsh conditions, including cosmic radiation, microgravity that induces muscle atrophy and bone density loss, and isolation and confinement potentially

resulting in psychological effects [12,13]. The physical and cognitive demands increase the risk of human error, which can be life-threatening in the unforgiving environment of space [14]. Moreover, missions beyond low Earth orbit, such as those to Mars, involve communication delays of up to 22 minutes one way, making real-time guidance from Earth impractical [15]. Missions will be longer, and Earth-independent operations will be essential. To overcome these obstacles, integrating automation, robots, and autonomy can enhance mission safety, efficiency, and success, extending the capabilities of human spaceflight to achieve more ambitious exploration goals [16–18].

In this context, it is important to distinguish between robots, automation, and autonomy. Robots are machines designed to perform tasks that may be hazardous or impractical for humans, ranging from simple repetitive actions to complex operations in extreme environments [17,19,20]. They can be remotely controlled or pre-programmed to execute specific functions. Automation involves systems operating with minimal human intervention by following predefined instructions, controllers, or algorithms to carry out tasks efficiently and consistently, reducing the need for constant human oversight but typically lacking the ability to adapt to unforeseen situations [21,22]. Autonomy, on the other hand, refers to systems capable of making independent decisions and adapting to new circumstances without human oversight, potentially utilizing artificial intelligence and machine learning to navigate unpredictable environments [23–25].

Human involvement varies across these technologies. In teleoperated robotic systems, humans are directly involved in controlling the machine, requiring seamless interfaces for real-time interaction. With automated systems, humans shift to roles focused on monitoring and intervention during exceptions, as the system handles routine tasks independently. Autonomous systems further minimize the need for human involvement during operations, placing greater emphasis on human roles in system design, oversight, and managing unexpected behaviors or emergencies. In space missions where communication delays can impede real-time control, autonomy becomes essential for tasks like navigation, maintenance, and exploration. Effective integration demands robust human-machine interfaces, clear communication protocols, and a great deal of trust to ensure mission success and safety [26,27].

These considerations become even more critical as space exploration advances toward long-duration endeavors that require human and robotic agents capable of independently maintaining the function of space systems, either autonomously or at least for extended periods. Operations such as maintaining space habitats, managing the Gateway functions, and undertaking Moon-to-Mars missions exemplify this shift toward extended missions [28,29]. These missions demand not only high-level intelligence but also sustained performance over prolonged periods, pushing the

limits of current human and robotic capabilities. Traditional methods that assess agent performance solely at the task level are inadequate for such complex applications because the resources consumed by agents—such as energy, time, and cognitive effort—are intrinsically linked to the utility they provide in achieving mission objectives [26,27,30]. Parameterized simulations that can account for the evolving habitat, random events, aging and degradation, and system interdependencies are more appropriate for exploring the trade space involved in mission design and assessing the associated logistical and resource requirements [26,31].

In addition to considering the agent capabilities and resources needed, the agents' availability to respond to unforeseen events should be assessed in early-phase mission design. Human agents are subject to physiological needs, including sleep cycles, nutrition, and fatigue management, which can impact their readiness and effectiveness [32]. Robotic agents, on the other hand, have limitations such as battery life, maintenance requirements, and potential system degradations that can affect their operational availability [33–35]. For instance, an astronaut's ability to perform emergency repairs might be compromised during designated rest periods, while a robot may be offline due to charging or software updates. A holistic perspective that considers the interplay between resources, utility, and availability is needed for early-phase decision-making, enabling mission planners to allocate tasks effectively between human and robotic agents [23,36,37].

With respect to these considerations, we develop and demonstrate a computational framework for early-stage mission design to enhance efficiency, safety, and overall success, paving the way for identifying regions where investments and research can have the greatest impact. Leveraging the CDCM rapid prototyping simulation tool, we consider autonomy that enable task performance within a SSH, specifically on the RA contrasted with the HA. A systematic comparison is performed to examine human and robot agents in the context of space missions by achieving the following key points. First, we introduce uncertainties into the modeling and simulation instead of following a deterministic process. Second, we consider the performance of human and robot agents in a mission-oriented study, i.e., we do not simply take a task-oriented perspective. Third, we consider the roles of the agents when they are interacting with an entire system instead of studying them in an isolated fashion.

We do not discuss the feasibility of technologies for realizing a robot agent that can provide the functional activities demanded in this paper. We use a recently developed robot as a basis to provide numerical specifications of the robot agent in this study. Providing a final answer to the questions raised in the beginning and further enabling humans and

robots to work side-by-side requires years of experimentation, data collection, and fundamental research, and it is beyond the scope of the present work. Herein, we form our model using currently available knowledge and data.

The proposed approach builds two independent scenarios for the HA and RA, respectively. Specifically, the models of the HA and RA include the daily schedule, the resources required, the task output they provide. When the SSH is damaged by a micrometeorite strike, tasks are assigned to agents for repairing the damaged systems, such as the structure, or power generation system. The goal is to keep the SSH in a safe condition to enable scientific research to be carried out. To evaluate this, we place an additional HS in both scenarios. The HS is only responsible for doing scientific research. In addition to using scientific research hours as the metric for indicating benefit, we use a modified version of equivalent system mass (M-ESM) to indicate the cost of using the HA and RA. The M-ESM accounts for mass, volume, crew time, power and cooling for maintaining temperature and pressure in the internal environment. Simulations run for each scenario individually to generate results, and conclusions can be drawn from those results.

Our approach can be used for a variety of aims, including mission design or agent selection. The space habitat is treated as a system of systems, currently including the human agent, robot agent, power generation, structure, health management, interior environment systems [31,38–40]. For each system, several states are defined to capture the characteristics necessary for the study. Each state is assigned a transition function to govern the simulation process. Then, the habitat state is the combination of all the states of all systems. Users can customize system design, numerical values, and models to realize specific scenarios. For instance, the space habitat can be configured in desired ways, with different types and numbers of systems, made-to-order interactions, adaptative modeling focus on selected system parts, and so on.

The paper is organized as follows. In Section II, we present the models of all space habitat systems in detail. Section III demonstrates a few illustrative examples to show how the approach can be used for addressing certain specific questions. We conclude with Section IV.

II. Approach

The technical approach is explained in Fig. 1. The study compares mission outcomes for two configuration choices, a HA and an RA, for a given task involving maintaining a smart space habitat. The habitat and its models will be explained in a subsequent section, along with the agent models. The primary purpose of this notional habitat is to conduct scientific research and the mission duration is ten years. Thus, the time that is available to do science is the performance metric used in our study. However, incidents can occur and cause significant disruption to the regular

operation of the space habitat. For example, structural damage to the habitat may be caused by a direct micrometeorite strike or by ejecta caused by a nearby strike. Thus, an emergency arises when a disruption happens in each scenario, and the agent must react to remedy the situation. To include uncertainty in the study, the occurrence of disruption events is random and governed by a probability distribution. Thus, the agents must react to each dynamic and unexpected emergency.

We construct two scenarios, as in Fig. 1. Scenario 1 employs an HA, and Scenario 2 uses an RA to perform repair tasks. Each scenario is further divided into three components of models that are the key elements defining the strategy. Scenario 1 has three possible configurations: 1A, 1B, and 1C. In 1A, the HA reacts to emergencies and performs the corresponding repair tasks. In 1B, we have an additional HS responsible for carrying out scientific research serving as a metric to evaluate the HA. Third, in 1C, the space habitat is configured to accommodate the HS and support its needs.

In Scenario 2, we also have three possible configurations: 2A, 2B, and 2C. In 2A, an RA takes the role of attending to emergencies. Version 2B is identical to 1B. In 2C, the overall configuration of the smart habitat is similar to that of 1C. Some specific changes are captured to reflect the needs and functions of different agents. For instance, to support RA, the habitat in Scenario 2 varies from Scenario 1 in that the power generation system is responsible for charging the RA's battery. Further details will be explained in Section II.B, Battery Modeling of RA.

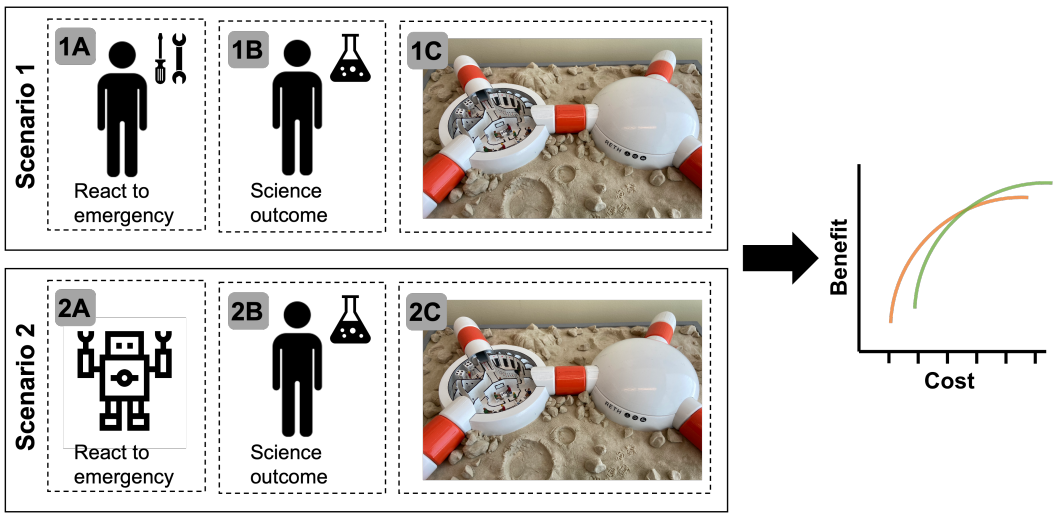


Fig. 1 Approach overview: Scenario 1 and Scenario 2 for evaluating the HA and the RA respectively.

We implement our model using the control-oriented dynamic computational modeling framework (CDCM) [31,41]. The CDCM is a modular framework that allows users to build a space habitat model focusing on explicitly capturing the causal relationships between the involved variables. The resulting models are represented as

computational graphs, which can be manipulated programmatically to achieve different goals [31,39]. Once Scenarios 1 and 2 are constructed, simulations are performed using the entire system encompassing the habitat systems, agents, and their interactions. The details of the system and the simulation will be explained in Section III.

For each scenario, an ensemble of simulations is performed to explore the impact of uncertainties. The overall results are evaluated in terms of benefit and cost. The benefit is quantified as the hours of scientific work generated over the mission by the HS with each scenario, as explained in Section II.C. Cost is quantified as the cost of the entire system measured by M-ESM when either the HA or the RA is included. Based on the results of the ensemble of realizations, conclusions about the choice of the agents are drawn.

In the following sections, we discuss the modeling of all systems and how we use the metrics to evaluate their performance.

A. Modeling of Systems in Scenario 1

The systems included in this SoS are modeled at different levels of fidelity, as shown in Fig. 2. A sufficient amount of detail must be included in the HA and HS models in this study's scope. Models designed with fewer details and shared between both scenarios include those for the structural, power generation, and health management systems. An interior environment model is included to capture the conditions inside the habitat. All the models are executed with a time step of one hour.

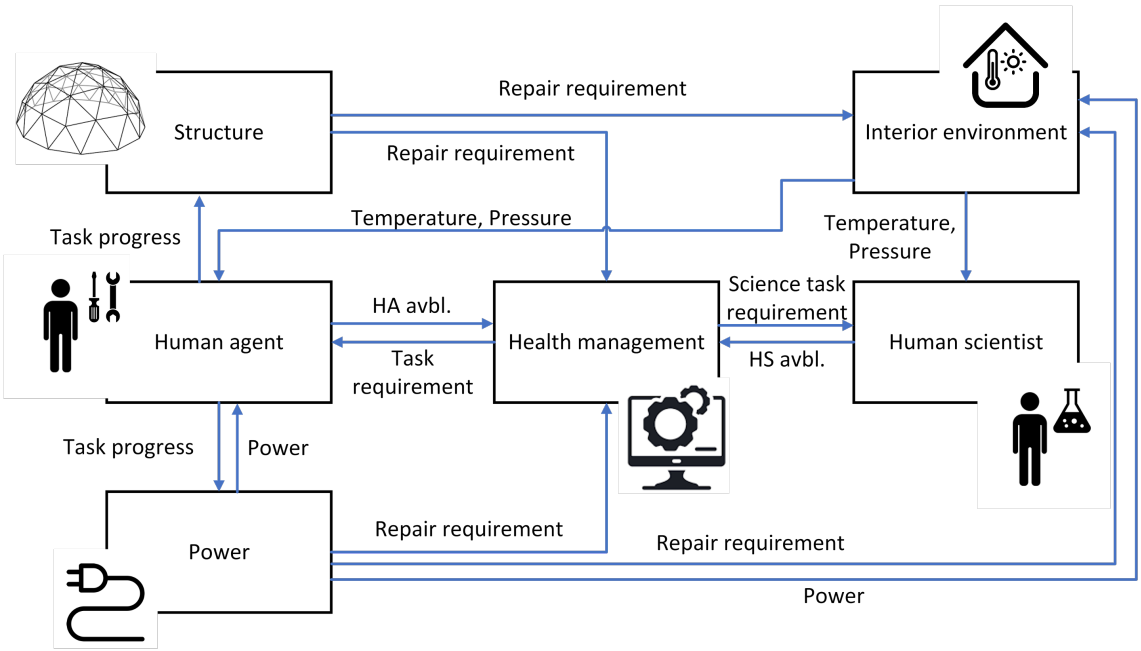


Fig. 2 Configuration of Scenario 1 (for evaluating the performance of the HA).

The following contents are discussed based on Scenario 1, and afterward, the discussion focuses on the different components in Scenario 2, specifically the RA.

1. Structural system modeling (ST)

ST represents the physical structural component of the habitat. As it is not the main attribute of this study, this model captures a disruption from a micrometeorite strike based on the probability of occurrence during each simulation time step. ST is damaged whenever a micrometeorite strike occurs in a simulation and requires repair by the HA (in Scenario 1). A damaged condition of the ST affects the interior environment (IE) by changing the ambient temperature and pressure until the repair is complete. The ST returns to nominal when the HA finishes a repair task. When the ST is under repair by the HA, it is unlikely, but possible, for the ST to be damaged again by another micrometeorite strike. The additional disruption also causes the current repair by the HA to return to zero progress. Relevant details are discussed in Sections II.A.3, the IE, and II.A.5, the HA. A more comprehensive demonstration of this behavior is provided in Section III.A through the detailed verification.

2. The power generation system modeling (PG)

In Scenario 1, the PG has a similar role as the ST, potentially being affected by a disruption and influencing the IE when there is damage. PG is subject to solar panel damage caused by a micrometeorite strike (MS) independent of the MS that happened to the ST. Two MS with the same given probability of occurrence affect the ST and the PG. When such an event occurs, the HA is responsible for repairing the PG. Other details are the same as the ST when it is subject to additional damage.

3. The interior environment modeling (IE)

The model of the IE governs the dynamics of the two states used for describing the interior volume of the habitat, ambient temperature, and pressure, $X_{3,t}^{0}$, and $X_{3,t}^{1}$. In the nominal condition of the habitat, both states are maintained at their optimal values. When the habitat transitions to an emergency condition due to the condition of the ST or/and the PG, the ambient temperature changes towards the temperature outside of the habitat. On the other hand, the ambient pressure always drops as the Moon's surface is a vacuum. When the habitat is repaired and returns to its nominal condition, these states return to their predefined set points. It should be noted that the values of ambient temperature and pressure influence all of the agents, the HA, the HS, and the RA. A safe range is defined in Section II.A.5 for the

two classes of human agents (the HA and the HS), and when the values of these two states fall outside of those ranges and would cause harm to the human agents, we declare that the mission fails, and terminate the simulation. The energy provided by the PG is used to support the IE when ambient temperature and pressure are not at their optimal values, which are the optimal values required by the HA, as discussed in Section II.A.5. Note that the two states also influence the performance of the HA while it is performing repair tasks, as discussed subsequently.

4. The health management system modeling (HMS)

The HMS is designed to assign the agent (the HA or the RA) to repair the damaged system. The HMS takes two inputs: the requirement from the ST or/and the PG and the agent's availability. If there is a requirement and simultaneously the agent is available, the HMS gives the corresponding task requirement to the agent. Otherwise, the task requirement is "None." When a repair task is in progress, the repair for the other system must wait until the ongoing task is finished. A specific scenario is when both the ST and the PG are under disruptions simultaneously, leading to task requirements for repairing the ST and the PG. In such a case, we prioritize the repair of the ST over the PG. The HMS first assigns the agent to repair the ST. Only when this task finishes is the agent sent to repair the PG.

5. The human agent modeling (HA)

The HA model is developed to capture details of a human agent while maintaining a space habitat. The model reflects the presence of the HA in the habitat and its role in performing repair tasks in emergency situations. The details of the HA are divided into several modules. These include the daily schedule, resource (oxygen, water, food), health, and task modules. Each module is modeled as a number of states for capturing the HA's initial values and transitions. For instance, a resource module is built for recording the resources consumed by the HA in each time step in the simulation. Moreover, the modules are not entirely separate from each other. Interactions in the transition functions can catch the interdependencies that exist between modules.

Daily schedule modeling

The model captures, at the highest level, the range of daily activities of the HA during a mission. These activities are required to support the basic functions of the HA, like eating and sleeping. Meanwhile, there should be a situation when the HA is performing tasks. The possible activities included are defined as:

1) **Sleeping**. This happens every 24 hours. This activity takes 8 hours, from 23:00 to 7:00. The HA does not sleep at other times.
2) **Eating**. This occurs thrice every 24 hours. Each meal takes 1 hour. The times are 7:00 to 8:00 for breakfast, then 12:00 to 13:00, and 18:00 to 19:00, respectively, for lunch and dinner.
3) **Exercising**. This activity lasts 3 hours every 24 hours, from 19:00 to 22:00.
4) **Idle**. Describes when the HA is not doing any other activities. This activity takes place in the time besides the time of all the other activities in the above, sleeping, eating, and exercising.
5) **Working**. Describes when the HA is doing repair tasks. As explained at the beginning of Section II. The HA is only designated to perform repair tasks for the ST and the PG. Herein, this status happens in a randomized manner, leading by the occurrence of the requirement of emergency tasks.

To distinguish between the activities that happen at fixed times during a day and those that are event-driven, we first define the state, the HA default status, $X_{5,t}^{0}$, which describes the routine status of the HA and what the HA is scheduled to do at time t. Depending on the disruption that can happen randomly during a simulation, "Working" is not considered in the range of the HA default status. Instead, "Working" is covered by the HA status, $X_{5,t}^{2}$. In this study, we assume that under some circumstances, a portion of the default activities, "Eating" or "Sleeping", can be skipped to some extent to yield that time for "Working" if needed for coping with emergencies. To decide whether the current default activity can be skipped, we consider the relative relationship between the current the HA health and predefined thresholds.

The details of the states describing the HA health will be explained in Section II.A, Health modeling. Here, we briefly explain how to decide when the HA is "Working". To begin with, we introduce the state of HA availability, $X_{5,t}^{1}$, which describes whether the HA is available for performing emergency tasks during a particular time step. We compare HA eating health with an eating threshold and HA sleeping health with a sleeping threshold. When both health terms are above their threshold, the HA is ready to skip "Eating" or "Sleeping" and react to emergencies. On the other hand, it is denoted as HA availability being True. Otherwise, we consider "Eating" is not skippable when eating health drops below its threshold, or/and a similar case is for "Sleeping." In this case, HA availability is set to False, representing that the HA is not available for any tasks at the time step. HA availability remains False until eating health or sleeping health rises again to be above the thresholds.

After introducing HA availability, it is straightforward to define HA status. Only when the HMS gives a task assignment, and HA availability is True, concurrently HA status is "Working." In other cases, the HA status follows the value of HA default status.

Resource modeling

Here, we model the simplified necessary resources to support life for the HA. These include oxygen, water, and food, each defined in terms of its mass and volume in the simulations. We use available data from the literature to capture the consumption of these three distinct resources. More specifically, we turn to data published and summarized from past space missions and generate probability distributions from them. Then, we use samples drawn from these distributions to determine the resources consumed in each realization.

1) **Oxygen consumption**. NASA lists typical steady-state values for the oxygen consumed in a vehicle environment [42], reporting a lower value of 0.518, a nominal value of 0.818, and an upper value of 5.67 kg/CM-D (crew member - day). We divide these values by 24 to the hour scale, kg/CM-H (crew member - hour), and use them as the basis of the model, indicating oxygen consumption per time step is not a fixed value. Because the nominal value is not at the center between the lower and upper values, we fit a skew normal distribution to capture the trend of oxygen consumption. The distribution for oxygen consumption in one hour is obtained as,

$$X_{5,t}^{3} \sim D(\alpha = 15.82, \xi = 0.015\ kg/CM\text{-}h, \omega = 0.11\, kg/CM\text{-}h). \quad (1)$$

2) **Water consumption**. NASA provides single values as the typical steady-state water usage rates for various missions [42]. The value for a mature planetary base is selected here, which is 9.82 kg/CM-D. We fit a normal distribution to represent the consumption value. The water usage rate per hour (0.41 kg/CM-H) is used as the mean value, with 5% and 95% percentile being 0.39 and 0.43 kg/CM-H (95% and 105% of 0.41 kg/CM-H). The distribution for water consumption in one hour is obtained as,

$$X_{5,t}^{4} \sim N(\mu = 0.41\ kg/CM\text{-}h, \sigma = 0.01\, kg/CM\text{-}h). \quad (2)$$

3) **Food consumption**. A typical 10-day menu is provided for short-term missions in space [42]. Each day, the mass of the food provided to a single crew member is given. We do not distinguish between different meals: breakfast, lunch, and dinner. All three meals are considered to follow the same distribution. The food is

measured before cooking or, in another sense, after dehydration. We fit a normal distribution to the set formed by the ten discrete food mass values (0.53, 0.56, 0.48, 0.42, 0.68, 0.46, 0.61, 0.39, 0.41, 0.56 kg/CM-Meal) through maximum likelihood estimation. The distribution for food consumption in one meal is obtained as,

$$X_{5,t}^{5} \sim N(\mu = 0.51\, kg/CM\text{-}Meal\,, \sigma = 0.09\, kg/CM\text{-}Meal). \quad (3)$$

In addition, constant energy usage is included to support the space suit when the HA is at "Working," as all the repairs are considered to happen outside of the habitat.

Health Modeling

HA health is modeled as a concept different from the everyday use of the term "health." We use health to describe the capability of the HA to perform assigned tasks. When health is at its maximum value, the HA is able to output the best performance when reacting to an emergency. When health decreases, the performance will correspondingly drop.

HA health is currently modeled as a product of four simplified states: Eating Health, Sleeping Health, Thermal Health, and Pressure Health. Each of the states ranges from 0 to 1 (0% to 100%), resulting in a single value for HA health between 0 to 1. During the simulation, all health state values are influenced by their corresponding factors (e.g., ambient temperature) and may fluctuate within the bounds, either increasing or decreasing over the simulation steps.

1) **Eating health**. This state reflects the relationship between the number of meals the HA has and their related health state. We consider the possible condition where the HA misses a number of meals to repair damaged systems and how this will influence its eating health. To build the model, we resort to studies to find the relationship between food deprivation and cognitive performance [43]. In turn, we treat food deprivation from the study as the number of meals missed and cognitive performance as eating health, affecting task performance. We adopt three cases from [43], 10%, 30%, and 50% of required consumption. These numerical values stand for the percentage of the required food consumed in the experiments, then one minus the percentage value, e.g., 1-10%, is the food missed. Neglecting the cases of food deprivation with 70% and 90%, because some amount of food deprivation may result in a performance increase of food deprivation, which we do not consider in this study. In each plot (10%, 30%, 50%), x is the number of days for the experiment, and y is the performance in %, ranging from 0 to 1. Here, 10% of required consumption is transferred to 10% of meals eaten, indicating 1-10% of meals missed. Then, we choose 10 points from each

percentage plot to form the dataset and fit a standard normal distribution to the formed dataset. A random sample from the distribution represents the change in eating health caused by one meal. This can be used for two cases: when the HA misses one meal, which leads to a decrease in eating health, or when the HA has a meal, it results in an increase in eating health if it is less than 100%. The random sample from the distribution serves as the amount of increase or decrease in eating health value. Then, the change of eating health per meal, $H_{HA,Eating}$, is expressed as,

$$H_{HA,Eating} \sim N(\mu = 0.0014\ meal^{-1}, \sigma = 0.0004\ meal^{-1}). \quad (4)$$

2) **Sleeping Health**. The hours of sleep per day are found to be among several factors that influence human cognitive performance [44]. From the literature [44], cognitive performance peaks when participants have 7 hours of sleep and continuously drops towards lower and higher hours of sleep. Nevertheless, a typical daily schedule of a crew member in deep space is recommended as 8.5 hours by NASA [42]. Given that the higher priority of deep space missions is always to weigh HA health over its performance, we choose 8 hours of sleep as the number in our study. The performance level at 8 hours is the highest value for cognitive performance [44], and truncate any values higher than that to 100%, and calculate any other values lower than that for the percentage of difference with respect to the value at 8 hours, and then form a dataset, and generate the distribution to the formed dataset. We only consider the data points with hours of sleep equal to or less than 8 hours [44]. Then, sleeping health transits in the realizations in the same way as eating health. When the HA misses one hour of "Sleeping" for an emergency, sleeping health drops by a value. When the HA has one hour of "Sleeping," sleeping health increases by a value if it is less than 100%. The values are random samples from the distribution built in this section. The distribution for the change of sleeping health per hour is given as,

$$H_{HA,Sleeping}(t) \sim N(\mu = 0.0014\ sleeping\text{-}hour^{-1}, \sigma = 0.0004\ sleeping\text{-}hour^{-1}). \quad (5)$$

3) **Thermal health**. In this study, three values can govern the behavior of the ambient temperature and the ambient pressure in a space vehicle or space habitat. They are an optimal value, a lower value and an upper value (hereafter, $p_{T,o}$, $p_{T,l}$ and $p_{T,u}$ for temperature, and $p_{P,o}$, $p_{P,l}$ and $p_{P,u}$ for pressure, respectively). At the optimal value of $p_{T,o}$, we assume that the HA is under the best condition of ambient environment in terms of ambient temperature. Thermal health, therefore, equals its maximum value in such circumstances. We will

see a drop in thermal health when the ambient temperature moves away from $p_{T,o}$ towards $p_{T,l}$ and $p_{T,u}$. The following model reflects the relationship between thermal health and ambient temperature. We pick the ambient temperature in a typical steady vehicle atmosphere as the reference, with as lower point of 291 K, a nominal point as 296 K, and an upper point of 300 K [42]. Sequentially, $p_{T,o}$, $p_{T,l}$ and $p_{T,u}$are set as 21, 18, and 27 °C, and thermal health is assigned to 1, 0.95, and 0.95 correspondingly. Then, we model the function of thermal health in the range of $p_{T,o}$ and $p_{T,l}$, and the range of $p_{T,o}$ and $p_{T,u}$ as two independent sigmoid functions [45]. Given the ambient temperature, $X_{3,t}^0$, at a time step, the function of thermal health is obtained as,

$$X_{5,t}^8 = \begin{cases} \frac{1}{1+e^{-2.35X_{3,t}^0+39.39}}, if 18 \le X_{3,t}^0 \le 21, \\ \frac{1}{1+e^{1.18X_{3,t}^0-34.59}}, if 21 < X_{3,t}^0 \le 27, \\ 0.95, otherwise. \end{cases} \quad (6)$$

Outside of $p_{T,l}$ and $p_{T,u}$, we set the values of $X_{5,t}^8$ to stay at 0.95. This is because when the ambient temperature is outside of this range, we consider the simulation as a failed realization, and to reflect that, a hefty penalty is added to the cost metric, which will be explained in Section II.C. Under the circumstance, the effect of ambient temperature on thermal health is not considered at the same level as in the normal condition (ambient temperature within the range of $p_{T,l}$ and $p_{T,u}$).

4) **Pressure health**. Like the modeling of thermal health, we refer to the ambient pressure in a typical steady vehicle atmosphere as lower point as 48 kPa, nominal point as 101 kPa, and upper point as 102.7 kPa [42]. These values, at this moment, are set as which of the setting points, $p_{P,o}$ as 101 kPa, $p_{P,l}$ as 48 kPa and $p_{P,u}$ as 102.7 kPa. Then, the function of pressure health is expressed as,

$$X_{5,t}^9 = \begin{cases} \frac{1}{1+e^{-0.13X_{3,t}^1+3.44}}, if 48 \le X_{3,t}^1 \le 101, \\ \frac{1}{1+e^{4.15X_{3,t}^1-429.18}}, if 101 < X_{3,t}^1 \le 102.7, \\ 0.95, otherwise. \end{cases} \quad (7)$$

Additionally, the lower point and upper point of ambient temperature (18 °C and 27 °C) and ambient pressure (48 kPa and 102.7 kPa) are treated as the safety range of the IE or the SSH. When either one is outside of the range, the SSH is considered in a hazardous state until the values are back to the safety range. This is applied to both Scenarios 1 and 2.

Task modeling

The process to finish a task is modeled by assuming that, during each time step, the agent (robot or human) can complete a percentage of the task, defined as task progress. When the amount reaches 100%, the task is finished. During each time step, there is a probability that the agent fails at performing the repair, in which case the progress at that time step stays the same as in the previous time step. The repair of damage to the ST and the PG, for both the HA and the RA, is modeled independently. To reflect specific repair procedures, varying task progress rates, and task success probability values are chosen for each system (the ST and the PG). The rate of each agent's progress at each time step and the probability for success at each step is based on the technique we choose to repair the damage and the related data, which will be discussed in Section III, illustrative examples.

6. The human scientist modeling (HS)

The HS is modeled almost identically to the HA, has the same nominal schedule, and uses resources in the same manner. The only discrepancy is in task assignments. Instead of reacting to emergency tasks, the HS is designed to perform scientific research. This contribution is then used for comparing the agents' performance in the two scenarios. During each time step that the habitat is in a safe condition (i.e., there are no emergency tasks to perform), the HS has a probability to successfully output a research hour (the probability is set as 50%). During emergencies, the HS will not generate research hours at all. Intuitively, this is meant to evaluate the ability of the HA (later for the RA) to keep the habitat in a functional condition. In this study, we envision that a functional condition is a condition suitable for conducting research.

B. Modeling of Systems in Scenario 2

Scenario 2 is set up for simulating and evaluating the performance of the RA, as shown in Fig. 3. To make both scenarios comparable for our purpose, the RA replaces the roles of the HA in Scenario 1. In contrast, the rest of the systems in Scenario 2 are replicas of the systems in Scenario 1. The only difference is that with Scenario 2, the PG model includes a function to supply power to the RA. Here, we will focus on the distinguishing feature of this model, the RA.

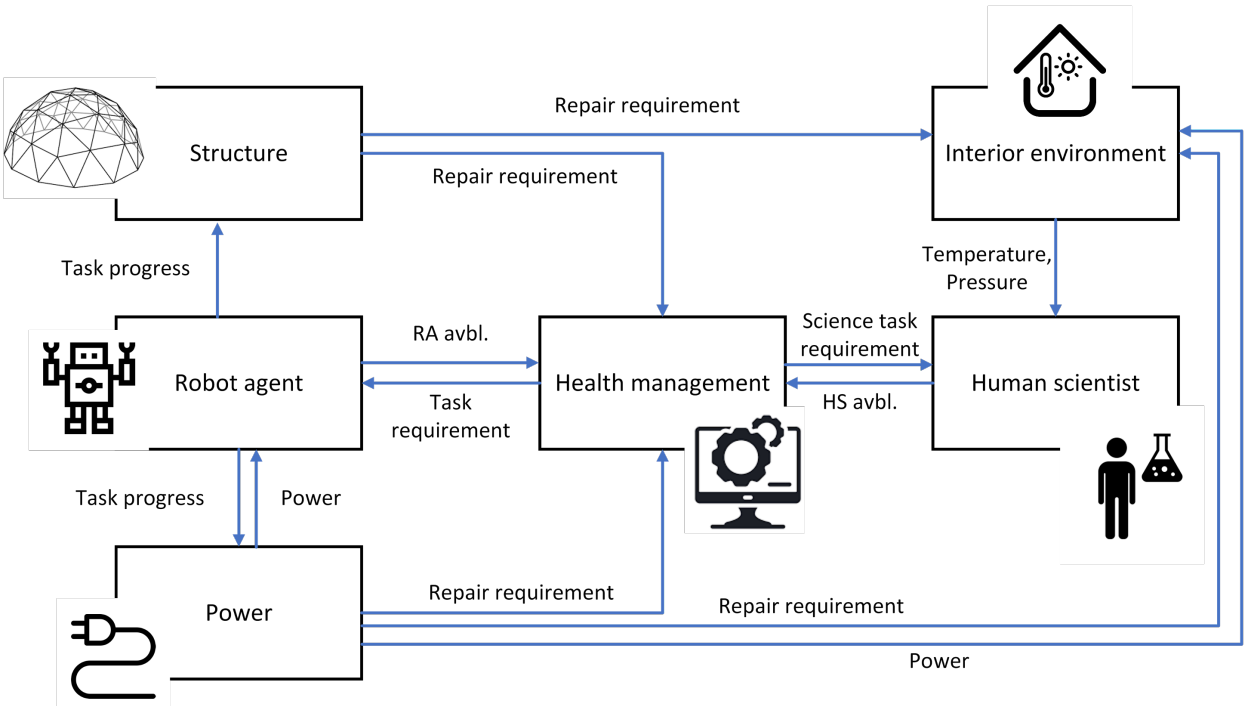


Fig. 3 Configuration of Scenario 2 (for evaluating the performance of RA).

1. The robotic agent modeling (RA)

In this study, the RA is modeled to reflect a hypothetic robot in a space habitat that can move within the habitat and carry out repair tasks while neglecting the discussion of whether the technology to support the capabilities is available. We limit the modeling to a relatively realistic level by referring to market-available robots for setting up the numerical values of the related physics of the RA [46]. Apart from the above, some unique features of the RA differ from those of the HA. For instance, the RA requires a battery to support its activities while the HA needs the support of oxygen, water, and food; the RA requires no "Sleeping" activity while the HA does, etc.

Daily schedule modeling

We define all the possible activities of the RA in a mission. All are event-based and thus do not happen in a regular period. Also, we consider the RA to be self-sufficient enough to carry out all the activities independently without additional human intervention. These activities are:

1) **Replacing**. describes when one of the RA's components is removed and a renewal is installed. This depends on whether the health of the RA's components is lower than their thresholds, which is caused by degradation over time.

2) **Charging**. describes when the RA connects to the habitat and draws electric power to till its battery. A battery is incorporated into the RA as a critical component, serving to store energy required for the RA's various activities. The battery needs charging to refill the energy and output power for supporting activities of the RA.
3) **Working**. describes when the RA is doing repair task. Like the modeling of the HA in Section II.A.5, this occurs when an emergency leads to a task requirement.
4) **Idle**. describes when the RA is at no other activities.

Some of the activities are coupled with the modeling details of the RA below. To be more specific, "Charging" is coupled with battery modeling. "Replacing" is coupled with motor degradation and battery degradation as in the modeling of RA health. "Working" is regulated in task modeling and is affected by RA health. Details are explained in the section below.

Battery modeling

A battery charged with a sufficient amount of energy is necessary to support the RA. Hereby, we model the battery of the RA with the functionalities of storing energy, taking in energy by "Charging," and outputting energy when "Working." During the simulation, the "Charging" activity is constantly given the highest priority due to its critical role in supporting the battery. "Charging" herein can happen during a repair task and between the occurrence of "Working." This does not indicate we value the condition of the RA over SSH. Instead, it simply suggests that the RA requires energy, resupplied by "Charging," to perform the repair tasks.

Drawn from the battery, a certain amount of energy is consumed for each time step when the RA is at "Working." To guarantee the left energy in the battery is sufficient to support the "Working" of the RA in the incoming time step, we set up a threshold value for determining when the RA switches to "Charging." When the energy in the battery is lower than such threshold, the RA goes to "Charging" activity regardless of the current condition of the space habitat. To ease the tension of "Charging" on the performance given by the RA, we also set the RA to charge its battery during "Idle" or "Replacing." However, a discrepancy exists between the two situations where the RA charges its battery to the full amount during "Charging." At the same time, the RA stops its battery charge during "Idle" or "Replacing" anytime when there is an emergency or working requirement.

Degradation and resources modeling

Over the long term of the mission, on a year scale, degradation of the RA needs to be taken into consideration. Two components of the RA are considered to bear a degradation over time: the battery and the motor(s). Their performance drops over time through usage and natural rest. To capture this, we model the degradation of the health of the battery and motor over time. Two individual degradation functions are built. And degradation has consequences. The health of the battery under the degradation curve directly affects the energy capacity or the maximum energy it can store. Consequently, it affects the performance that the RA can provide for "Working" by reducing the time for work and increasing the frequency for "Charging." Meanwhile, the health of the battery and the motor are considered as coefficients to reduce the task speed and the task success probability of the RA.

The degradation curve of the battery is modeled by an exponential function [47]. It starts as 100% (or 1) at time being 0 and continuously drops as time increases. The curve is featured by a marking point, where we pick from the reference that the battery health will drop to approximately 90% at two years of usage [47]. We obtain the degradation function governing the battery health as

$$X_{6,t}^{5} = 2^{-t/116800}. \tag{8}$$

Similarly, the degradation curve of motors of the RA is modeled as a PF curve (potential failure – functional failure) [48]. Motor health ranges from 100% (1) to 0% (0). To get the exact curve, we refer to the fact that a motor is normally expected to last for 30,000 hours of usage [49]. Then, the degradation function for motor health of the RA is defined as

$$X_{6,t}^{6} = 1 - (t/30000)^{2}. \tag{9}$$

Following the degradation curves, when the health of the battery and motor drops below selected thresholds, they are replaced. Replacements are defined as the resources needed by the RA.

Task modeling

The RA is modeled in the same way as the HA in the context of performing tasks, described by the task speed and task success probability output by the RA. The details are not repeated here.

C. Metrics

Cost and benefit are used to compare the two agents in the next section. Two metrics are used, as shown in table 1 and follows

Table 1 Summary of the values used for M-ESM calculation

	Mass (kg)	Volume (m^3)	Factor for Volume (kg/m^3)	Power (kW)	Factor for power (kg/kW)	Cooling (kW)	Factor for cooling (kg/kW)	Crew-time or robot time (CM-h/y)	Duration of mission (y)	Factor for crew-time or robot time (kg/CM-h)
				Scenario 1						
HA [42,50]	90	3.42	9.16	$X_{5,t}^{13}$	76					
HA – oxygen [51]	$6.77*X_{5,t}^{3}$	$0.0045*X_{5,t}^{3}$	9.16							
HA – water [52]	$1.032*X_{5,t}^{4}$	$0.011*X_{5,t}^{4}$	9.16							
HA – food [42]	$1.17*X_{5,t}^{5}$	$0.0027*X_{5,t}^{5}$	9.16							
HS [42,50]	90	3.42	9.16							
HS – oxygen [51]	$6.77*X_{7,t}^{3}$	$0.0045*X_{7,t}^{3}$	9.16							
HS – water [52]	$1.032*X_{7,t}^{4}$	$0.011*X_{7,t}^{4}$	9.16							
HS – food [42]	$1.17*X_{7,t}^{5}$	$0.0027*X_{7,t}^{5}$	9.16							
IE [42]				$X_{3,t}^{3} + X_{3,t}^{5}$	76	$X_{3,t}^{3}$	102			
ST and PG [42]								$X_{5,t}^{14}$	10	1.50
				Scenario 2						
RA [42,46]	272	0.60	9.16	$X_{6,t}^{12}$	76					
HS [42,50]	90	3.42	9.16							
HS – oxygen [51]	$6.77*X_{7,t}^{3}$	$0.0045*X_{7,t}^{3}$	9.16							
HS – water [52]	$1.032*X_{7,t}^{4}$	$0.011*X_{7,t}^{4}$	9.16							
HS – food [42]	$1.17*X_{7,t}^{5}$	$0.0027*X_{7,t}^{5}$	9.16							
IE [42]				$X_{3,t}^{3} + X_{3,t}^{5}$	76	$X_{3,t}^{3}$	102			
ST and PG [42]								$X_{6,t}^{11}$	10	1.50

1) Cost: The M-ESM is chosen as the metric for denoting the cost of each scenario. To work with the models developed in this paper, computations are based on the agent models and the systems that interact with them, ensuring that only the necessary components are calculated. The M-ESM is calculated following the equations [53], which consider mass, volume, crew-time, power needs, and cooling needs. Note that the specific values are difficult to obtain, so in some cases, assumptions are used and are noted where they occur. The values we use for modeling and, in turn, calculating the M-ESM are summarized in Table 2. These values are divided into those relevant to Scenario 1 and those for Scenario 2. In Scenario 1, we start with the HA

calculations, including the agent's mass and volume. We assume that consumed resources, such as oxygen, water, and food, are shipped from the Earth. As the resources being consumed accumulate over time, the numerical values in Table 2 correspond to oxygen, water, and food per kg of the consumed resources. To obtain the total mass and volume for the consumed resources over the whole simulation, we multiply by the amount of the consumed resources, denoted by $X_{5,t}^{3}$ for oxygen, $X_{5,t}^{4}$ for water, and $X_{5,t}^{5}$ for food to the values. We are currently not including many details of the systems required for processing the resources, such as tanks, pumps, food preparation, etc. The procedure used for the HS is similar. The power consumption for supporting the spacesuit of the HA during tasks is included as $X_{5,t}^{12}$. We also include the power to control the ambient temperature and ambient pressure, respectively, $X_{3,t}^{2}$ and $X_{3,t}^{4}$. Then $X_{3,t}^{2}$, $X_{3,t}^{4}$ and $X_{5,t}^{12}$ are divided by mission time length to obtain the power requirement for each term, as $X_{3,t}^{3}$, $X_{3,t}^{5}$ and $X_{5,t}^{13}$, and the average over a mission time length of the power term for controlling ambient temperature is treated as cooling power requirement. Additionally, we include values for the ST and the PG because task inputs to the HA are generated. Herein, crew-time, $X_{5,t}^{14}$, for performing the task is considered. The same logic is followed for Scenario 2 and will not be discussed in detail. The citations used for obtaining the values are provided in the table. Specifically, the Factor for Volume is chosen as 9.16, and the Factor for crew-time is 1.50 because the calculation relates to the Moon [42]. In the end, a penalty value is added to the M-ESM if the SSH is in a hazardous state determined by ambient temperature and ambient pressure, as discussed in Sections II.A.3 and II.A.5, Health Modeling.

2) Benefit: One of the primary goals for future deep space missions is to "support scientific research" [54,55]. Towards this direction, we use science research hours (SRH) as the metric for measurement of the benefit of a given scenario. SRH is the accumulated time that HS works on research or simply is in the "Working" state. This value is mainly governed by the task modeling of the HS in Section II.

III. Illustrative Examples

With the developed approach, a range of illustrative examples are studied to demonstrate how to use the models developed for comparing mission outcomes with either the HA or the RA. The first example serves as a demonstration, which the subsequent examples are built upon for establishing the baseline for comparing the agents' performance at a mission-level. Moving forward, the second example illustrates the impact of varying task speed and success rate on

the outcomes. The final example is to demonstrate how to explore technology investments through an evaluation of enabling alternate RA's "Charging" methods on the results.

In the examples, Scenarios 1 and 2 are each simulated for 100 realizations to consider the uncertainties captured by the model of the SoS. The simulated mission lasts for ten years. The simulation time step is 1 hour. MS are introduced as disruptions to the SSH on the Moon. In this study, each MS event can directly cause corresponding system damage, while more complex relationships between the MS and the damage it causes will be studied later. Unless otherwise stated, the configurations mentioned above, along with the models detailed in Section II, are applied throughout the examples.

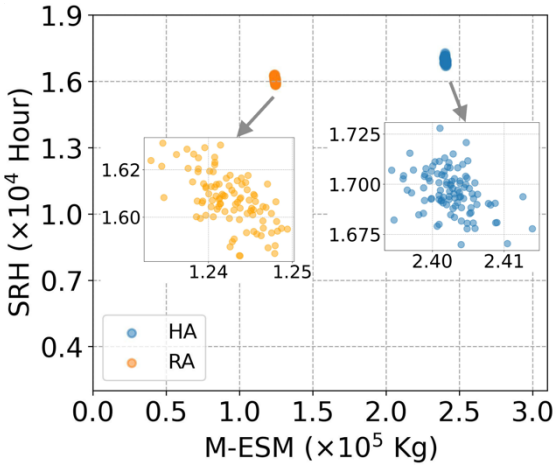
A. Example I: Simulation Outcomes at a Mission Level

We examine the overall outcomes at a mission level, as depicted in Fig. 4. In Fig. 4(a), we delve into the case where MS randomly occurs and the average damage frequency is chosen as 0.4% per hour (3 MS in one month). This frequency applies to both the ST and the PG, although independently. Here, the results with each of the two agents naturally form two distributions. Scenario 1 (with the HA) results are portrayed in blue and fall in the upper right corner, while Scenario 2 (with the RA) results are shown in orange and are clustered in the upper left corner of the figure. In the enlarged plots, each point represents one realization, as in Fig. 4(b) and (c). Each single point reflects the consequence of the interplay of various stochastic factors, encompassing the occurrence of the MS, the task performance by the agents, and more. Clearly, the HA has a larger cost (the M-ESM) due to the required resources to support the HA, while it yields more science hours. Both metrics decrease for the RA. The RA requires about half of the cost of the HA and generates about 94% of the benefits of the HA.

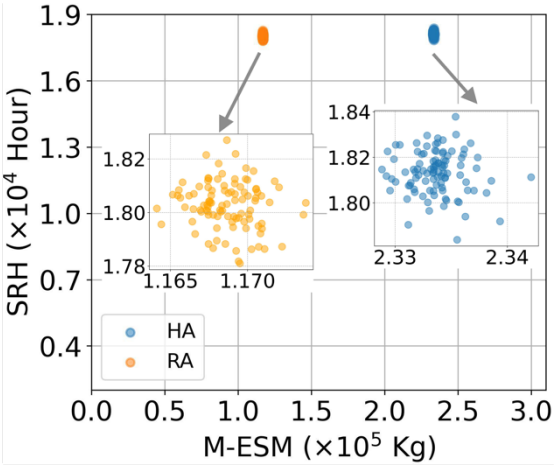
We further investigate the same question with varying damage frequencies, specifically 0.04% and 4% (0.3 and 30 MS in one month). These variations naturally result in decreased or increased workload for the agents, with outcomes illustrated in Fig. 4(b) and (c). The case where the MS frequency is set as 0.04% generates an increased SRH due to less frequent repair tasks. Consequently, it is evident that when the probability of an emergency is reduced significantly, the benefits (i.e., the SRH in Scenario 2) of the RA start to align with those of the HA. In comparison to the 0.4% case, the SRH rises by about 11% for the HA and 12% for the RA. However, it is essential to note that the HA requires a higher M-ESM with respect to the RA in Fig. 4(b). While the likelihood of emergencies triggered by natural events, like the MS, hardly varies drastically, the variability in the outcomes can be attributed to the differing levels of resilience exhibited by the systems within the habitat. For example, the case in which the ST is under the

influence of a less frequent MS can be treated as a more resilient ST and, therefore, is less likely to be damaged under a given likelihood of the MS. This suggests that designing and constructing more resilient systems will influence the comparison between the HA and the RA. In Fig. 4(c), where the MS frequency increases to 4%, we observe that SRH generated by both the HA and the RA drops comparing to other frequencies. At the same time, the M-ESM of both the RA and the HA increases. Although a 4% probability of the MS is not likely, we could still extrapolate this outcome to consider that with a different, but frequent, emergency, the HA would outperform the RA in terms of the SRH (the larger, the better) by an obvious advantage, but with a cost almost twice as much as the RA.

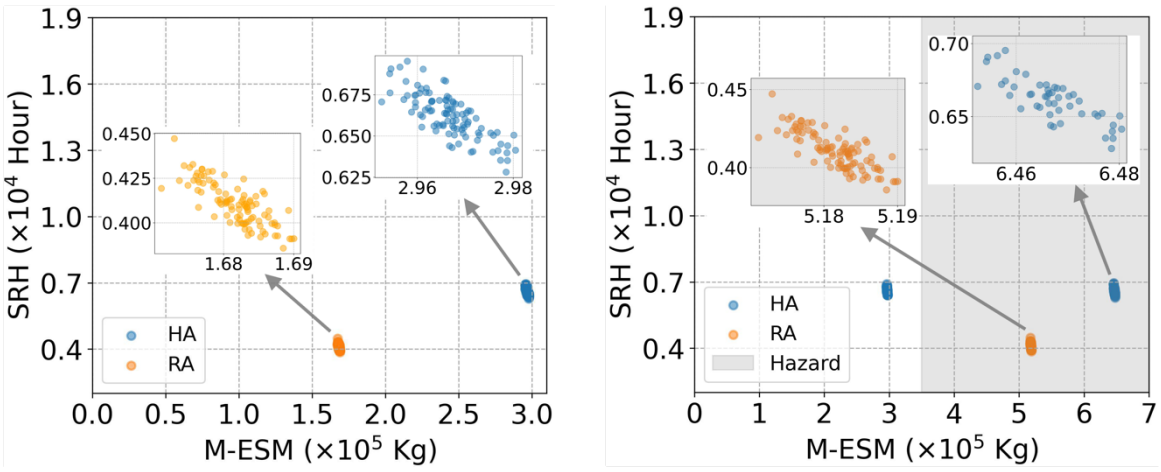
It is worth noting that in both Fig. 4(a) and (c), each group of results forms a similar arrangement from upper left to lower right direction. This is because the uncertainties are mainly due to the occurrence of emergencies or task requirements. As more frequent tasks are needed, the cost increases, encompassing the relative terms in the M-ESM calculation (i.e., power consumption, resource consumption, crew-time), while simultaneously reducing generated the SRH, as the space habitat is more frequently under an emergency condition, stopping the "Research" activity of the HS. Moreover, the pattern of both agents becomes more obvious, as in Fig. 4(c) compared to Fig. 4(a). We infer that with more frequent MS, this pattern is more evident. This is also the reason that no such phenomenon is observed in Fig. 4(b), as the task requirement in this case does not yet overwhelm the capability of the agents.



(a) Damage frequency of 0.4%



(b) Damage frequency of 0.04%



(c) Damage frequency of 4%

(c) Damage frequency of 4%, with a penalty

Fig. 4 Overall outcomes of ten-year simulations for analyzing mission success with the HA and the RA under MS disruption events with frequencies of 0.4%, 0.04% and 4%.

When the repair task by the agents takes a significant amount of their time, for example, when the MS frequency is 4%, the habitat is more likely to be in a hazardous state, which causes the science outcome to be low, as shown in Fig. 4(c). To understand this, we add a penalty cost (an extreme large value) to the M-ESM for each scenario when the SSH is considered in a hazardous state. This is evaluated by the ambient temperature and pressure, as explained in Section II.A.5. No single realization of the HA and the RA are penalized when the MS frequencies are set as 0.04% and 0.4%. Therefore, we only display the remaining case when the MS frequency is 4% for the same realization of simulations as above with the SRH but cost metric, including the penalty value. In the figure, we denote the hazardous zone by grey; therefore, when the result of a realization falls in the grey region, it indicates that the space habitat is in a hazardous state at some point in the mission. From Fig. 4(d), the deterioration is obvious. Scenario 1 with the HA has 50% of the realizations being hazardous. Moreover, all the realizations for the RA are considered unsuccessful in terms of maintaining the safety of the space habitat. This indicates that with a relatively high level of dangerous cases, which corresponds to an MS rate of 4%, or one MS every 25 hours, there is a significant chance that the HA is not able to fulfill the mission, while the RA may not be able to cope with the case at all. By comparison, the resistance to increasingly frequent disruptions is higher from the HA to the RA.

B. Example II: Studying the Effect of Varying Task Performance

In this example, we study the consequences of varying task performance, building upon the results established in Section III.A. We parameterize two variables: task speed coefficient, s, and task success probability coefficient, r. These coefficients are multipliers to change task speed and task success probability, respectively, to alter the task

performance of the agents within the simulation. Each coefficient is varied from 0.4 to 2 in increments of 0.1, giving 17 values. A value of 1 is nominal, and is used in Example I. Meanwhile, we associate the variables with a corresponding change in the numerical values of the M-ESM to reflect the additional cost for increasing or decreasing the task speed and task success. The additional cost is associated with advancing the technologies for supporting the HA (e.g., human augmentation robotics and smart wearable devices) or building better RAs. Intuitively, higher task performance requires an additional cost. Then, we run the same simulations as in Section III.B for each configuration, each representing a unique combination of task coefficient, task probability coefficient, and damage frequency, encompassing 867 configurations.

The results are presented in Fig. 5. We categorize the results into six groups for graphical clarity. For example, consider the case of an RA with a damage frequency of 4%. This case corresponds to the region filled by deep purple in the left lower corner of the figure and all points belonging to that region, denoted Region 4. Each individual point represents the simulation result for a specific configuration. A total of 100 realizations are conducted, and each data point is the mean over these realizations. Results for the HA are in blue, and the RA is in orange. For an RA with a damage frequency of 4%, the data points span from over 100,000 kg to over 400,000 kg in the M-ESM direction and from below 17,000 hours to about 19,000 hours in the SRH direction. This dispersion is attributed to the varied task performance configuration implemented for the RA under a single damage frequency. Some configurations yield improved performance, while others fall short, incurring a penalty in the form of increased M-ESM. During simulations, the penalty is added to the M-ESM only once if necessary. Consequently, for one realization, as in Fig. 4 in Section III.B, there are two sets of results, without penalty or with penalty. In contrast, focusing again on the RA with a damage frequency of 4%, we observe a range of scattered data points positioned between the leftmost and rightmost groups. This result can be attributed to the fact that this is mean data point. Across the 100 realizations to simulate each combination, some realizations remain penalty-free while others incur penalties. When transformed to mean points, the M-ESM values with a penalty are placed within the intermediate region, resulting in the observed scatter.

Upon comprehending the distinct regions, we look at the relative relationship between the different groups in Fig. 5. Overlapping regions indicate that with specific agent configurations, either two agents or one agent with different damage frequencies can each yield comparable outcomes. For the same damage frequency, it states that the HA's region is positioned to the right of the figure compared to the RA. However, these regions are not entirely separated,

as overlapping regions exist between the HA and the RA across different damage frequencies. On the other hand, when assessing different damage frequencies, the results are arranged from the bottom to the top of the figure, corresponding to the decreased damage frequency. This aligns with our observations from Section III.B, where a less frequent MS rate results in increased SRH for both agents. Under closer examination, the RA with a damage frequency of 4% (Region 6) overlays with the HA with a damage frequency of 4% (Region 3). RA with a damage frequency of 0.4% (Region 5) shares two partial regions, respectively, with the HA with a damage frequency of 4% and 0.4% (Regions 2 and 3). It can be interpreted that, for the same agent, it is unlikely to have its performance under damage frequencies of 4% and 0.4% be identical to each other, given the varying performance capability. However, regarding the damage frequency of 0.4% and 0.04%, overlap exists, as shown in the enlarged plot for the HA (Regions 1 and 2). The same is true for the RA. Moreover, the HA and the RA can deliver comparable outcomes by changing their task speed or/and task probability, even under two relatively frequent disruptions (the RA with a frequency of 0.4% compared to the HA with a frequency of 4%, Region 5 to 3).

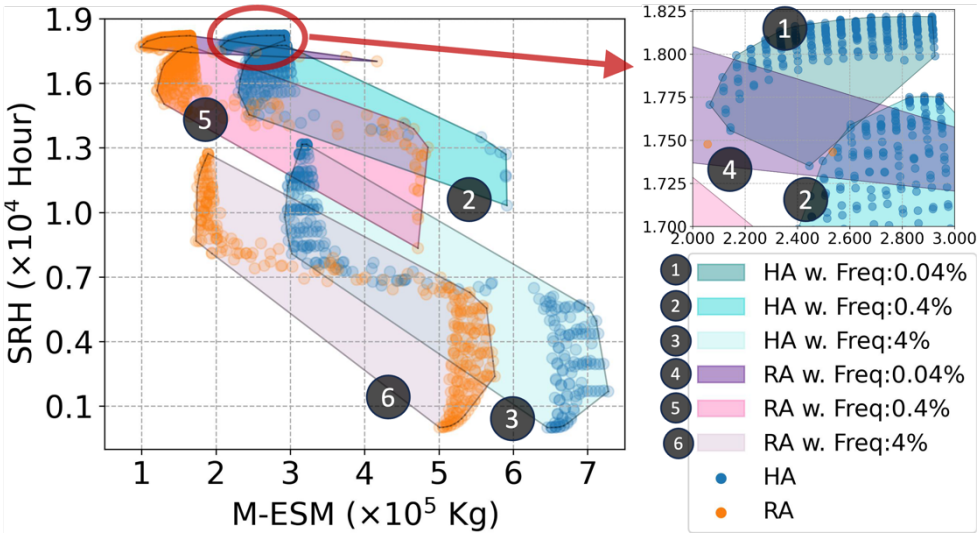


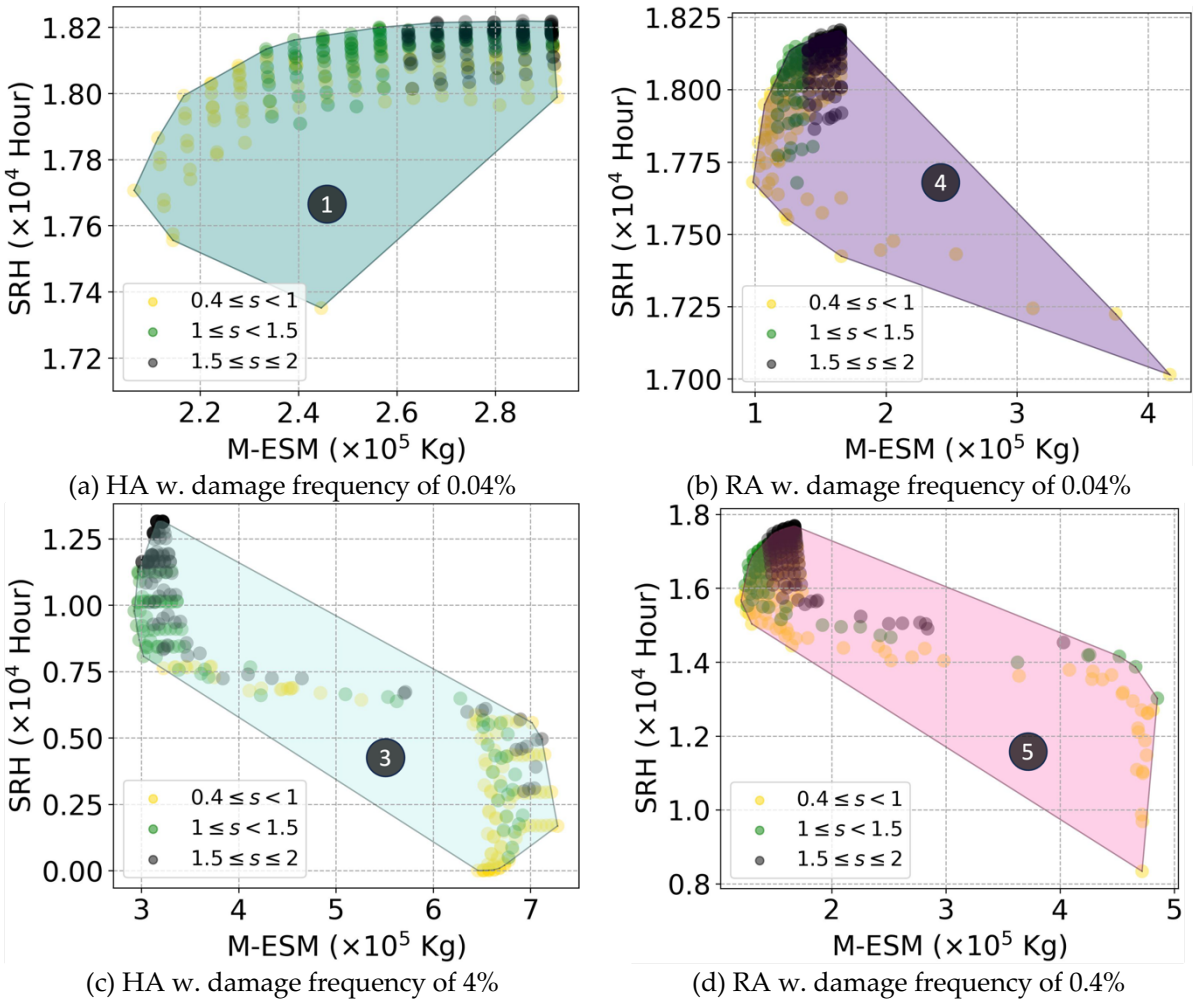
Fig. 5 Outcomes with varying task speed and task success rate for the HA and the RA: Region 1, the HA with disruption frequency of 0.04%; Region 2, the HA with 0.4%; Region 3, the HA with 4%; Region 4, the RA with 0.04%; Region 5, the RA with 0.4%; Region 6, the RA with 4%.

For a more elaborate examination, we focus our attention on comparing outcomes within a given region. For region 1, the outcomes are detailed in Fig. 6(a). The majority of the points are grouped in the upper left, leaving one yellow point below. The line-up on the left and upper boundary forms the Pareto front of points in Region 1. On this front, we observe that more benefit requires higher cost. From left to right, the same amount of cost increase gives a reduced gain of benefit. We further categorize the outcomes by the values of s. Three intervals are selected: less than 1 (depicted in yellow), from 1 to 1.5 (depicted in green), and no less than 1.5 (depicted in black). Outcomes in black are

driven to the right side, while green points stay in the center of the Pareto front, leaving yellow points in the very left. Points hold similar trends below the Pareto front, though further away from the front, more yellow points and less green or black points are observed, as compared to those on the front.

Similar outcomes are observed for the RA with a damage frequency of 0.04% or Region 4, as in Fig. 6(b). The points in the upper left exhibit the same pattern, with the Pareto front being more compact than in Fig. 6(a). The relative placements of the points within three intervals hold the same relationship. However, more yellow points are scattered across Region 4 to its right side. This outcome means that the agents' task speed or task success probability cannot cope with the increased MS frequency, leading to a hazardous state in the space habitat. Again, higher M-ESM and less SRH can be expected, while the amount of the change is determined by the specific improvement of the agents and the disruption frequency.

The HA with a damage frequency of 4% (Region 3) and the RA w. damage frequency of 0.4% (Region 5) is analyzed next. In Fig. 6(c) and (d), intricate distributions of the points emerge as we move away from the left boundaries. Besides yellow points, a substantial number of points within the two higher intervals are also present. This suggests that as the damage frequency rises from 0.04% to 0.4% and 4%, the increased task speed cannot guarantee the simulation will be free from penalties. Remember that any point not in the upper left of each region signifies that the mission can fail and fall into the penalty zone. This trend is further supported by the points along the right border of Fig 6(c) and (d). Primarily, yellow points, a number of green points and one black point lie in the right in Fig 6(d), whereas with a damage frequency of 4% in Fig. 6(c), a more significant presence of green and black points is seen in the same positions. Note these outcomes result from the coupling of task speed coefficient and task success probability coefficient. With the same task speed, agents can deliver varying levels of performance depending on the task success probability and the damage frequency condition. When damage frequency is low, a low task success probability alone is likely to ensure the level of the mission outcome, as in the scatter of yellow points in Fig. 6(a) and (b). Otherwise, it requires the interplay of speed and success probability in higher damage frequency conditions.



(a) HA w. damage frequency of 0.04%

(b) RA w. damage frequency of 0.04%

(c) HA w. damage frequency of 4%

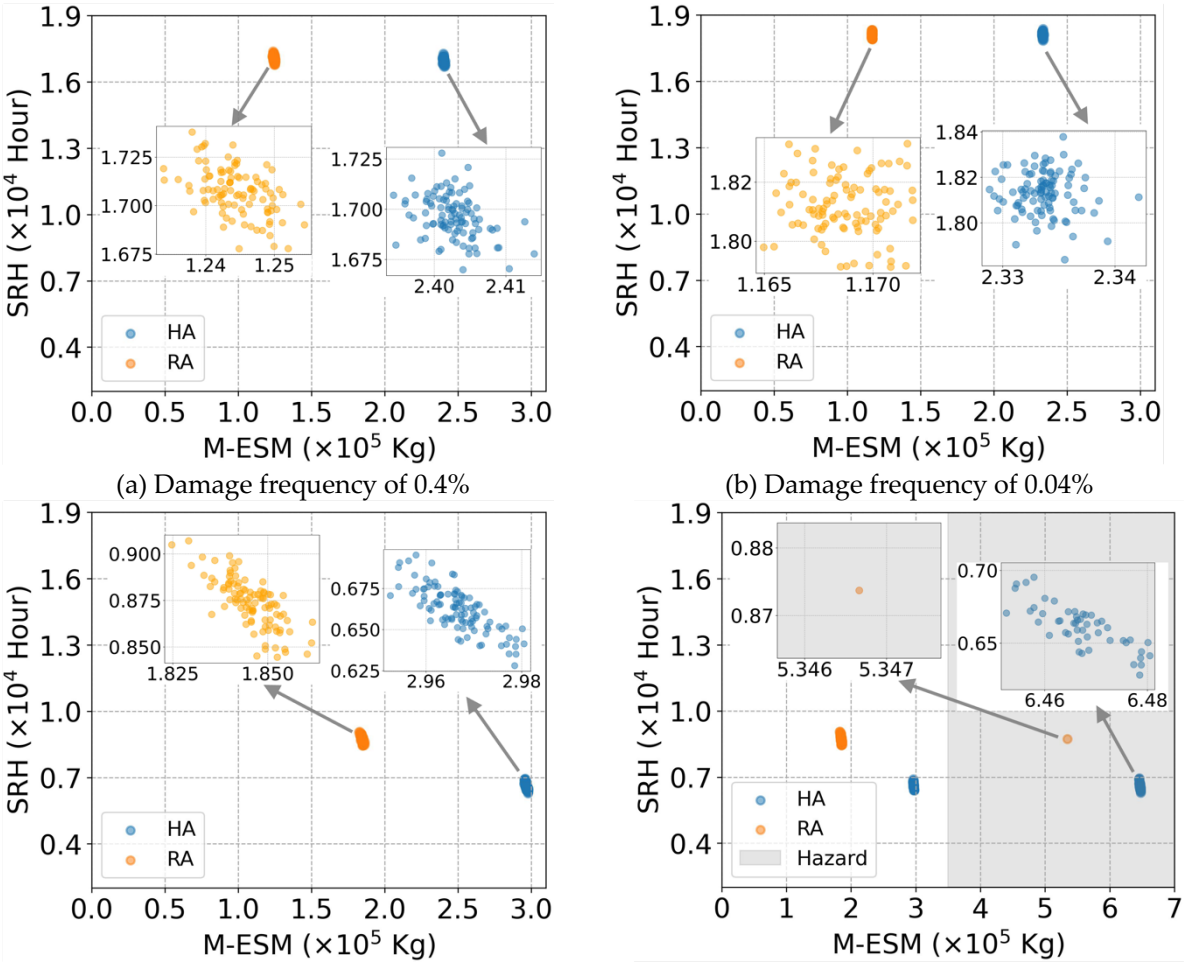
(d) RA w. damage frequency of 0.4%

Fig. 6 Close examination of outcomes with varying task speed coefficient denoted by *s*: Region 1, the HA with 0.04%; Region 3, the HA with 4%; Region 4, the RA with 0.04%; Region 5, the RA with 0.4%.

C. Example III: Studying the Effect of Remote Wireless Charging on the Roles of the RA

During the detailed process of RA repairs, the RA repeatedly switches between "Working" and "Charging". Inevitably, this limits its performance. Electrical power is the essential resource that the RA relies on to move from one location to a target location, identify its surroundings, pick up objects, etc. Herein we use a battery concept to store the electrical power to provide it to the RA. One possible improvement is to increase the battery capacity, though the extra weight potentially may reduce the speed or efficiency of the RA. Alternatively, a promising technology that may be available in the near future is wireless charging [56]. Approaches are being developed to charge a battery without the need for physical connections or cables. The field is heading toward realizing remote wireless charging when over-the-air or no-contact charging. In this example, we focus on exploring the benefits and costs of investing in this technology in the RA. By enabling the battery to be charged constantly, the RA avoids all "Charging" activities

and can generate more science outcomes. Skipping the details of the technology itself, we consider a method to examine its potential benefits. In Fig. 7, we compare the simulation results with the modified RA to those of the same HA model. We see that in Fig. 7(b), when damage frequency is 0.04%, the RA does not show any obvious advantages to the HA. When the damage frequency increases to 0.4%, in Fig. 7(a), an improvement in science outcome is generated by the RA over the HA. Furthermore, if we increase the frequency to 4%, as in Fig. 7(c), the improvement is obvious. The benefit of the RA rises from 4000 hours, as in Fig. 7(c), to 8750 hours with the modification. Moreover, the benefit of the RA surpasses the HA in this situation. Moreover, the chance of falling into a hazardous state reduces from 100%, as in Section III.B, to 1%, as shown in Fig. 7(c). However, it should be noted that taking advantage of wireless charging can add a cost for design, installation, which is not yet considered here. If those data were known, we could include them. However, wireless charging is an up-and-coming technology.



(a) Damage frequency of 0.4%

(b) Damage frequency of 0.04%

(c) Damage frequency of 4%

(d) Damage frequency of 4%, with a penalty

Fig. 7 Overall outcomes with remote wireless charging to support the RA.

IV. Conclusions

Having a method to study the role of agents in the context of space missions holds great importance due to the evolving landscape of space exploration. As humanity ventures toward more complex and extended missions, such as the establishment of permanent habitats on the Moon, the roles of agents, human or robotic, become a substantial consideration. Allocating roles to the agents is central to mission success, safety, and efficiency.

In this paper we introduce the stochastic models and the computational framework that facilitates such comparisons for decisions, and can expanded for more specific studies in future phases. A key achievement demonstrated here is the ability to quantitatively analyze outcomes under customized configurations, including customized choice of space habitat configuration, models, and numerical values for best reflecting the target research question. In addition, introducing randomness or stochastic elements into models and simulations allows for capturing the inherent variability and uncertainty of the space habitat system, leading to more robust and realistic predictions and analyses. Another significant contribution is our approach to treating human and robotic agents as elements within a system of systems, which offers a novel perspective in the study of human and/or robot in space missions. Additionally, this work establishes a foundation for modeling various aspects of human and robotic agents, such as quantifying agent health and resource consumption, as discussed in Section II. These models will serve as foundations to models of varying fidelities to enable other research objectives. Furthermore, modules not covered in this paper can be integrated into this framework using the modeling logic presented.

In addition, this paper demonstrates that determining the optimal strategy for agent performance is a complex and compounded decision-making process influenced by multiple stochastic interrelated factors, where variations in the frequency and intensity of external disruptions, combined with the capabilities of the agents and task requirements, can significantly alter conclusions about which agent performs better. This complexity further increases when additional factors, such as material properties for structural repairs, environmental conditions, resource availability, required technologies, and mission setup, are considered, necessitating a powerful analytical framework to navigate the intricate considerations involved.

The project's findings support important decisions: using stochastic disruptions to identify the likelihood of mission success, supporting dynamic mission planning by enabling simulations to be reconfigured from any intermediate state, identifying key technologies for future space missions that are worthy of targeted investment, and facilitating the

analysis of intermediate values throughout the rich time history outcomes of each mission, such as logistical requirements. These capabilities enhance our understanding and preparation for future space missions.

It is worth noting that the approach and illustrative examples are based on the accessible data, which do not necessarily reflect the actual agent capabilities in the future space mission. The data collection process for human agent and robot agent, which can be deployed in a space environment alone, can span several years. Given this temporal reality, conducting such comprehensive comparison studies after all data and knowledge have been amassed becomes improbable. Along the journey, our approach can serve as a compelling tool for rationalizing the acquisition of specific data, allowing for the prioritization of data importance and the strategic focus of research and technology development efforts.

Appendix – Supplemental Material

Table A1 Structural system modeling (ST)

Attribute	Notation	Description	Value
Name	ST		
id	1		
Coupling inputs	$X_{5,t}^{10}$	Task progress	
Control inputs	-	-	
External disturbances	-	-	
States	$X_{1,t}^{0}$	Damage happened to the ST	{True, False}
	$X_{1,t}^{1}$	Requirement for repairing from ST	{True, False}
Parameters	$\theta_{1,t}^{0}$	Damage frequency	
Coupled parameters	-	-	
State transition functions		$X_{1,t}^{0} \sim \text{Bernoulli}(\theta_{1,t}^{0})$ $X_{1,t}^{1}$: Table A1-1	

Table A1-1 State transition function of requirement for repairing from ST ($X_{1,t}^{1}$)

Output	$X_{1,t}^{1}$
Pseudo code	$X_{1,t}^{1} = f(t)$: if $X_{1,t}^{0} ==$ True: #new damage happens during repair $X_{1,t}^{1} =$ True $X_{5,t}^{10} = 0$ #set progress to 0 if $X_{5,t}^{10} == 1$ #task is finished $X_{1,t}^{1} =$ False

Table A2 Power generation system modeling (PG)

Attribute	Notation	Description	Value
Name	PG		
id	2		
Coupling inputs	$X_{5,t}^{10}$	Task progress	
Control inputs	-	-	
External disturbances	-	-	
States	$X_{2,t}^{0}$	The damage happened to the PG	{True, False}
	$X_{2,t}^{1}$	Requirement for repairing from PG	{True, False}
Parameters	θ_2^0	Damage frequency	
Coupled parameters	-	-	
State transition functions		$X_{2,t}^{0} \sim \text{Bernoulli}(\theta_2^0)$ $X_{2,t}^{1}$: Table A2-1	

Table A2-1 State transition function of requirement for repairing from PG ($X_{2,t}^{1}$)

Output	$X_{2,t}^{1}$

Pseudo code	$X_{2,t}^{1} = f(t)$:
	if $X_{2,t}^{0}$ == True: #new damage happens during repair
	  $X_{2,t}^{1} =$ True
	  $X_{5,t}^{10} = 0$ #set progress to 0
	if $X_{5,t}^{10} = 1$ #task is finished
	  $X_{2,t}^{1} =$ False

Table A3 Interior environment modeling (IE)

Attribute	Notation	Description	Value
Name	IE		
id	3		
Coupling inputs	$X_{1,t}^{1}$	Requirement for repairing from ST	
	$X_{2,t}^{1}$	Requirement for repairing from PG	
External disturbances	-	-	
States	$X_{3,t}^{0}$	Ambient temperature	
	$X_{3,t}^{1}$	Ambient pressure	
	$X_{3,t}^{2}$	Accumulate energy required by ambient temperature	
	$X_{3,t}^{3}$	Averaged energy required by ambient temperature	
	$X_{3,t}^{4}$	The energy required by ambient pressure	
	$X_{3,t}^{5}$	Averaged energy required by ambient pressure	
Parameters	θ_{3}^{0}	Default ambient temperature	21
	θ_{3}^{1}	Default ambient pressure	101
Coupled parameters	-	-	
State transition functions		$X_{3,t}^{0}$: Table A3-1	
		$X_{3,t}^{1}$: Table A3-2	
		$X_{3,t}^{2}$: Table A3-3	
		$X_{3,t}^{3} = X_{3,t}^{2}/t$	
		$X_{3,t}^{4}$: Table A3-4	
		$X_{3,t}^{5} = X_{3,t}^{4}/t$	

Table A3-1 State transition function of ambient temperature ($X_{3,t}^0$)

Output	$X_{3,t}^0$
Pseudo code	$X_{3,t}^0 = f(t)$: if $X_{1,t}^1$ == True or $X_{2,t}^1$ == True: #repair requirement $T = 249 + 52 * cos\left(\frac{2*pi*t}{29.5306*24} - \frac{pi}{4}\right) - 273.15$ $X_{3,t}^0 = X_{3,t-1}^0 + 0.01 * \left(T - X_{3,t-1}^0\right)$ # temperature changes else: $X_{3,t}^0 = \text{round}\left(X_{3,t}^0 + 0.9 * \left(\theta_3^0 - X_{3,t-1}^0\right)\right)$ #recover temperature

Table A3-2 State transition function of ambient pressure ($X_{3,t}^1$)

Output	$X_{3,t}^1$
Pseudo code	$X_{3,t}^1 = f(t)$: if $X_{1,t}^1$ == True or $X_{2,t}^1$ == True: #repair requirement $X_{3,t}^1 = X_{3,t-1}^1 * (1 - 0.01)$ #pressure drops else: $X_{3,t}^1 = \text{round}\left(X_{3,t}^1 + 0.9 * \left(\theta_3^1 - X_{3,t-1}^1\right)\right)$ #recover pressure

Table A3-3 State transition function of ambient temperature required energy ($X_{3,t}^2$)

Output	$X_{3,t}^2$
Pseudo code	$X_{3,t}^2 = f(t)$: if $X_{3,t}^0$!= 27: $X_{3,t}^2 = X_{3,t-1}^2 + 0.55$

Table A3-4 State transition function of ambient pressure required energy ($X_{3,t}^4$)

Output	$X_{3,t}^4$
Pseudo code	$X_{3,t}^4 = f(t)$: if $X_{3,t}^1$!= 101: $X_{3,t}^4 = X_{3,t-1}^4 + 0.01$

Table A4 Health management system modeling (HMS)

Attribute	Notation	Description	Value
Name	HMS		
id	4		
Coupling inputs	$X_{1,t}^{1}$	Requirement for repairing from ST	
	$X_{2,t}^{1}$	Requirement for repairing from PG	
	$X_{5,t}^{10}$	Human agent availability	
	$X_{6,t}^{1}$	Science agent availability	
Control inputs	-	-	
External disturbances	-	-	
States	$X_{4,t}^{0}$	Task requirement	{None, ST, PG}
	$X_{4,t}^{1}$	Science task requirement	{None, Science}
Parameters	-	-	
Coupled parameters	-	-	
State transition functions		$X_{4,t}^{0}$: Table A4-1	
		$X_{4,t}^{1}$: Table 4-2	

Table A4-1 State transition function of task requirement ($X_{4,t}^{0}$)

Output	$X_{4,t}^{0}$

Pseudo code	$X_{4,t}^{0} = f(t)$:
	if $X_{5,t}^{10}$ == True:
	  if $X_{1,t}^{1}$ == True: #repair structure
	  $X_{4,t}^{0}$ = "ST"
	  else if $X_{2,t}^{1}$ == True: #repair power
	  $X_{4,t}^{0}$ = "PG"
	else:
	  $X_{4,t}^{0}$ = "None"

Table A4-2 State transition function of science task requirement ($X_{4,t}^{1}$)

Output	$X_{4,t}^{1}$

Pseudo code	$X_{4,t}^{1} = f(t)$:
	if $X_{5,t}^{10}$ == True and $X_{1,t}^{1}$!= True and $X_{2,t}^{1}$!= True:
	  $r \sim U(0,1)$
	  if $r \geq 0.5$:
	  $X_{4,t}^{1}$ = "Science"
	else:
	  $X_{4,t}^{1}$ = "None"

Table A5 Human agent modeling (HA)

Attribute	Notation	Description	Value
Name	HA		
id	5		
Coupling inputs	$X_{3,t}^{0}$	Ambient temperature	
	$X_{3,t}^{1}$	Ambient pressure	
	$X_{4,t}^{0}$	Task requirement	{None, ST, PG}
Control inputs	-	-	
External disturbances	-	-	
States	$X_{5,t}^{0}$	HA default status	
	$X_{5,t}^{1}$	HA availability	{True, False}
	$X_{5,t}^{2}$	HA status	
	$X_{5,t}^{3}$	HA oxygen consumption	
	$X_{5,t}^{4}$	HA water consumption	
	$X_{5,t}^{5}$	HA food consumption	
	$X_{5,t}^{6}$	HA eating health	[0, 1]
	$X_{5,t}^{7}$	HA sleeping health	[0, 1]
	$X_{5,t}^{8}$	HA thermal health	[0, 1]
	$X_{5,t}^{9}$	HA pressure health	[0, 1]
	$X_{5,t}^{10}$	HA health	[0, 1]
	$X_{5,t}^{11}$	Task progress	[0, 1]
	$X_{5,t}^{12}$	HA energy consumption	
	$X_{5,t}^{13}$	Averaged HA energy consumption	
	$X_{5,t}^{14}$	Crew-time	
Parameters	θ_5^0	HA default status parameters	
	θ_5^1	HA eating health threshold	
	θ_5^2	HA sleeping health threshold	
	θ_5^3	HA oxygen parameters: [skewness, mean, standard deviation]	
	θ_5^4	HA water parameters: [mean, standard deviation]	
	θ_5^5	HA food parameters: [mean, standard deviation]	
	θ_5^6	HA eating parameters [mean, standard deviation]	
	θ_5^7	HA sleeping parameters [mean, standard deviation]	
	θ_5^8	HA temperature parameters	
	θ_5^9	HA pressure parameters	
	θ_5^{10}	HA task speed	
	θ_5^{11}	HA task success probability	
Coupled parameters	-	-	
State transition functions		$X_{5,t}^{0}$: Table A5-1	
		$X_{5,t}^{1}$: Table A5-2	
		$X_{5,t}^{2}$: Table A5-3	
		$X_{5,t}^{3}$: Table A5-4	
		$X_{5,t}^{4}$: Table A5-5	
		$X_{5,t}^{5}$: Table A5-6	

$X_{5,t}^{6}$: Table A5-7
$X_{5,t}^{7}$: Table A5-8
$X_{5,t}^{8}$: Table A5-9
$X_{5,t}^{9}$: Table A5-10
$X_{5,t}^{10} = X_{5,t}^{6} * X_{5,t}^{7} * X_{5,t}^{8} * X_{5,t}^{9}$
$X_{5,t}^{11}$: Table A5-11
$X_{5,t}^{12}$: Table A5-12
$X_{5,t}^{13} = X_{5,t}^{13}/t$
$X_{5,t}^{14}$: Table A5-13

Table A5-1 State transition function of HA default status ($X_{5,t}^{0}$)

Output	$X_{5,t}^{0}$

Pseudo code	$X_{5,t}^{0} = f(t)$:
	if $\theta_5^0[0] < t\%24 \leq \theta_5^0[1]$:
	$X_{5,t}^{0}$ = "Sleeping"
	else if $\theta_5^0[2] < t\%24 \leq \theta_5^0[3]$ or $\theta_5^0[4] < t\%24 \leq \theta_5^0[5]$ or $\theta_5^0[6] < t\%24 \leq \theta_5^0[7]$:
	$X_{5,t}^{0}$ = "Eating"
	else if $\theta_5^0[8] < t\%24 \leq \theta_5^0[9]$:
	$X_{5,t}^{0}$ = "Exercising"
	else:
	$X_{5,t}^{0}$ = "Idle"

Table A5-2 State transition function of HA availability ($X_{5,t}^{1}$)

Output	$X_{5,t}^{1}$

Pseudo code	$X_{5,t}^{1} = f(t)$:
	if $X_{5,t}^{6} \geq \theta_5^1$ and $X_{5,t}^{7} \geq \theta_5^2$: #working over default activities
	$X_{5,t}^{1}$ = True
	else:
	if $X_{5,t}^{6} < \theta_5^1$ and $X_{5,t}^{7} \geq \theta_5^2$:
	var = {$X_{5,t}^{0}$!= "Eating"}
	else if $X_{5,t}^{6} \geq \theta_5^1$ and $X_{5,t}^{6} < \theta_5^2$:
	var = {$X_{5,t}^{0}$!= "Sleeping"}
	else:
	var = {$X_{5,t}^{0}$!= "Eating"} and {$X_{5,t}^{0}$!= "Sleeping"}
	if var == True:
	$X_{5,t}^{1}$ = True
	else:
	$X_{5,t}^{1}$ = False

Table A5-3 State transition function of HA status ($X_{5,t}^{2}$)

Output	$X_{5,t}^{2}$

Pseudo code	$X_{5,t}^{2} = f(t)$:
	if $X_{4,t}^{0}$!= "None":
	$X_{5,t}^{2}$ = "Working"
	else:
	$X_{5,t}^{2} = X_{5,t}^{0}$

Table A5-4 State transition function of HA oxygen consumption ($X_{5,t}^{3}$)

Output	$X_{5,t}^{3}$

Pseudo code	$X_{5,t}^{3} = f(t)$:
	if $X_{5,t}^{2}$ == "Working" or "Exercising":
	  sample ~ D($\alpha = 1.2 * \theta_5^3[0], \xi = \theta_5^3[1], \omega = \theta_5^3[2]$)
	  $X_{5,t}^{3} = X_{5,t-1}^{3}$ + sample
	else:
	  sample ~ D($\alpha = \theta_5^3[0], \xi = \theta_5^3[1], \omega = \theta_5^3[2]$)
	  $X_{5,t}^{3} = X_{5,t-1}^{3}$ + sample

Table A5-5 State transition function of HA water consumption ($X_{5,t}^{4}$)

Output	$X_{5,t}^{4}$

Pseudo code	$X_{5,t}^{4} = f(t)$:
	if $X_{5,t}^{2}$ == "Working" or "Exercising":
	  sample ~ D($\alpha = 2, \xi = \theta_5^4[0], \omega = \theta_5^4[1]$)
	  $X_{5,t}^{4} = X_{5,t-1}^{4}$ + sample
	else:
	  sample ~ N($\mu = \theta_5^4[0], \delta = \theta_5^4[1]$)
	  $X_{5,t}^{4} = X_{5,t-1}^{4}$ + sample

Table A5-6 State transition function of HA food consumption ($X_{5,t}^{5}$)

Output	$X_{5,t}^{5}$

Pseudo code	$X_{5,t}^{5} = f(t)$:
	if $X_{5,t}^{2}$ == "Eating":
	  if $X_{5,t}^{10} < 1$:
	  sample ~ D($\alpha = 2, \xi = \theta_5^5[0], \omega = \theta_5^5[1]$)
	  else:
	  sample ~ N($\mu = \theta_5^5[0], \delta = \theta_5^5[1]$)
	  $X_{5,t}^{5} = X_{5,t-1}^{5}$ + sample

Table A5-7 State transition function of HA eating health ($X_{5,t}^{6}$)

Output	$X_{5,t}^{6}$

Pseudo code	$X_{5,t}^{6} = f(t)$:
	if $X_{5,t}^{0}$ == "Eating" and $X_{5,t}^{2}$ == "Working":
	  sample ~ N($\mu = \theta_5^6[0], \delta = \theta_5^6[1]$)
	  $X_{5,t}^{6} = X_{5,t-1}^{6}$ − sample
	else if $X_{5,t}^{0}$ == "Eating" and $X_{5,t}^{2}$ == "Eating":
	  sample ~ N($\mu = \theta_5^6[0], \delta = \theta_5^6[1]$)
	  $X_{5,t}^{6} = X_{5,t-1}^{6}$ + sample
	$X_{5,t}^{6}$ = min(1,max(0, $X_{5,t}^{6}$))

Table A5-8 State transition function of HA sleeping health ($X_{5,t}^{7}$)

Output	$X_{5,t}^{7}$

Pseudo code	$X_{5,t}^{7} = f(t)$:
	if $X_{5,t}^{0}$ == "Sleeping" and $X_{5,t}^{2}$ == "Working":
	sample ~ N($\mu = \theta_5^7[0], \delta = \theta_5^7[1]$)
	$X_{5,t}^{7}$ =$X_{5,t-1}^{7}$ − sample
	else if $X_{5,t}^{0}$ == "Sleeping" and $X_{5,t}^{2}$ == "Sleeping":
	sample ~ N($\mu = \theta_5^7[0], \delta = \theta_5^7[1]$)
	$X_{5,t}^{7} = X_{5,t}^{7}$ + sample
	$X_{5,t}^{7}$ = min(1,max(0, $X_{5,t}^{7}$))

Table A5-9 State transition function of HA thermal health ($X_{5,t}^{8}$)

Output	$X_{5,t}^{8}$

Pseudo code	$X_{5,t}^{8} = f(t)$:
	if $18 < X_{3,t}^{0} \leq 21$:
	$X_{5,t}^{8} = \frac{1}{1+e^{-2.35X_{3,t}^{0}+39.39}}$
	else if $21 < X_{3,t}^{0} \leq 27$:
	$X_{5,t}^{8} = \frac{1}{1+e^{1.18X_{3,t}^{0}-34.69}}$
	else:
	$X_{5,t}^{8} = 0.95$

Table A5-10 State transition function of HA pressure health ($X_{5,t}^{9}$)

Output	$X_{5,t}^{9}$

Pseudo code	$X_{5,t}^{9} = f(t)$:
	if $48 < X_{3,t}^{1} \leq 101$:
	$X_{5,t}^{9} = \frac{1}{1+e^{-0.13X_{3,t}^{1}+3.44}}$
	else if $101 < X_{3,t}^{1} \leq 102.7$:
	$X_{5,t}^{9} = \frac{1}{1+e^{4.15X_{3,t}^{1}-429.18}}$
	else:
	$X_{5,t}^{9} = 0.95$

Table A5-11 State transition function of HA task progress ($X_{5,t}^{11}$)

Output	$X_{5,t}^{11}$

Pseudo code	$X_{5,t}^{11} = f(t)$:
	if $X_{5,t}^{2}$ == "Working":
	$r \sim U(0,1)$
	if $r \geq \theta_5^{11}[X_{4,t}^{0}] * X_{5,t}^{10}$:
	$X_{5,t}^{11}[X_{4,t}^{0}] = X_{5,t-1}^{11}[X_{4,t}^{0}] + \theta_5^{10}[X_{4,t}^{0}] * X_{5,t}^{10}$ #update by task speed
	else:
	$X_{5,t}^{11}[X_{4,t}^{0}] = X_{5,t-1}^{11}[X_{4,t}^{0}]$

Table A5-12 State transition function of HA energy consumption ($X_{5,t}^{12}$)

Output	$X_{5,t}^{12}$
Pseudo code	$X_{5,t}^{12} = f(t)$: if $X_{5,t}^{2}$ == "Working": $X_{5,t}^{12} = X_{5,t-1}^{12} + 0.117$

Table A5-13 State transition function of HA crew-time ($X_{5,t}^{14}$)

Output	$X_{5,t}^{14}$
Pseudo code	$X_{5,t}^{14} = f(t)$: if $X_{5,t}^{2}$ == "Working": $X_{5,t}^{14} = X_{5,t-1}^{14} + 1$

Table A6 Robotic agent modeling (RA)

Attribute	Notation	Description	Value
Name	RA		
Id	6		
Coupling inputs	$X_{4,t}^{0}$	Task requirement	
Control inputs	-	-	
External disturbances	-	-	
States	$X_{6,t}^{0}$	RA availability	{True, False}
	$X_{6,t}^{1}$	RA status	
	$X_{6,t}^{2}$	RA battery charge	[0, 1]
	$X_{6,t}^{3}$	RA battery capacity	
	$X_{6,t}^{4}$	RA energy consumption	
	$X_{6,t}^{5}$	RA battery health	
	$X_{6,t}^{6}$	RA motor health	
	$X_{6,t}^{7}$	RA health	
	$X_{6,t}^{8}$	RA battery replacements	
	$X_{6,t}^{9}$	RA motor replacements	
	$X_{6,t}^{10}$	RA task progress	[0, 1]
	$X_{6,t}^{11}$	RA time	
	$X_{6,t}^{12}$	Averaged RA energy consumption	
Parameters	θ_{6}^{0}	RA battery charge threshold	
	θ_{6}^{1}	RA energy charge and consumption parameters	
	θ_{6}^{2}	RA battery default capacity	
	θ_{6}^{3}	RA battery replace threshold	
	θ_{6}^{4}	RA battery replacement	
	θ_{6}^{5}	RA motor replace threshold	
	θ_{6}^{6}	RA motor replacement	
	θ_{6}^{7}	RA task speed parameters	
	θ_{6}^{8}	RA task success parameters	
Coupled parameters	-	-	
State transition functions		$X_{6,t}^{0}$: Table A6-1	
		$X_{6,t}^{1}$: Table A6-2	
		$X_{6,t}^{2}, X_{6,t}^{4}$: Table A6-3	
		$X_{6,t}^{3} = \theta_{6,t}^{1} * X_{6,t}^{5}$	
		$X_{6,t}^{5} = 2^{-t/(2*365*24/0.15)}$	
		$X_{6,t}^{6} = 1 - \left(\frac{t}{30000}\right)^{2}$	
		$X_{6,t}^{7} = X_{6,t}^{5} * X_{6,t}^{6}$	
		$X_{6,t}^{8}$: Table A6-4	
		$X_{6,t}^{9}$: Table A6-5	
		$X_{6,t}^{10}$: Table A6-6	
		$X_{6,t}^{11}$: Table A6-7	
		$X_{6,t}^{12} = X_{6,t}^{4}/t$	

Table A6-1 State transition function of RA availability ($X_{6,t}^{0}$)

Output	$X_{6,t}^{0}$

Pseudo code	$X_{6,t}^{0} = f(t)$:
	if $X_{6,t}^{2} \geq \theta_{6}^{0}$ and $X_{6,t}^{5} \geq \theta_{6}^{3}$ and $X_{6,t}^{6} \geq \theta_{6}^{5}$:
	$X_{6,t}^{0}$ = True
	else:
	$X_{6,t}^{0}$ = False

Table A6-2 State transition function of RA status ($X_{6,t}^{1}$)

Output	$X_{6,t}^{1}$

Pseudo code	$X_{6,t}^{1} = f(t)$:
	if $X_{4,t}^{0}$!= "None":
	$X_{6,t}^{1}$ = "Working"
	else:
	if $X_{6,t}^{5} < \theta_{6}^{3}$ or $X_{6,t}^{6} < \theta_{6}^{5}$:
	$X_{6,t}^{1}$ = "Updating"
	else:
	if $X_{6,t}^{2} < \theta_{6}^{0}$:
	$X_{6,t}^{1}$ = "Charging"
	else:
	$X_{6,t}^{1}$ = "Idle"

Table A6-3 State transition function of RA battery charge ($X_{6,t}^{2}$) and RA energy consumption ($X_{6,t}^{4}$)

Output	$X_{6,t}^{2}$, $X_{6,t}^{4}$

Pseudo code	$X_{6,t}^{2}, X_{6,t}^{4} = f(t)$:
	if $X_{6,t}^{1}$ == "Working":
	$X_{6,t}^{2} = X_{6,t-1}^{2} - \theta_{6}^{1}$[Working]
	else:
	if $X_{6,t}^{1}$ == "Charging":
	$\theta_{6}^{0} = 1$
	$X_{6,t}^{2} = X_{6,t-1}^{2} + \theta_{6}^{1}$[Charging]
	$X_{6,t}^{4} = X_{6,t-1}^{4} + \theta_{6}^{1}$[Charging]
	if $X_{6,t-1}^{2} < 1$:
	$X_{6,t}^{2} = X_{6,t-1}^{2} + \theta_{6}^{1}$["Charging"]
	$X_{6,t}^{4} = X_{6,t-1}^{4} + \theta_{6}^{1}$[Charging]
	$X_{6,t}^{2}$ = min(max($X_{6,t}^{2}$,0),1)
	if $X_{6,t-1}^{2} = 1$:
	$\theta_{6}^{0} = 0.4$

Table A6-4 State transition function of RA battery replacements ($X_{6,t}^{8}$)

Output	$X_{6,t}^{8}$
Pseudo code	$X_{6,t}^{8} = f(t)$: if $X_{6,t}^{5} < \theta_{6}^{3}$: $X_{6,t}^{8} = X_{6,t-1}^{8} + \theta_{6}^{4}$

Table A6-5 State transition function of RA motor replacements ($X_{6,t}^{9}$)

Output	$X_{6,t}^{9}$
Pseudo code	$X_{6,t}^{9} = f(t)$: if $X_{6,t}^{6} < \theta_{6}^{5}$: $X_{6,t}^{9} = X_{6,t-1}^{9} + \theta_{6}^{6}$

Table A6-6 State transition function of RA task progress ($X_{6,t}^{10}$)

Output	$X_{6,t}^{10}$

Pseudo code	$X_{6,t}^{10} = f(t)$:
	if $X_{6,t}^{1}$ == "Working":
	$r \sim U(0,1)$
	if $r \geq \theta_6^8[X_{4,t}^0] * X_{6,t}^7$: #task success rate
	$X_{6,t}^{10}[X_{4,t}^0] = X_{6,t-1}^{10}[X_{4,t}^0] + \theta_6^7[X_{4,t}^0] * X_{6,t}^7$ #update by task speed
	else:
	$X_{6,t}^{10}[X_{4,t}^0] = X_{6,t-1}^{10}[X_{4,t}^0]$

Table A6-7 State transition function of RA time ($X_{6,t}^{11}$)

Output	$X_{6,t}^{11}$
Pseudo code	$X_{6,t}^{11} = f(t)$: if $X_{6,t}^{1}$ == "Working: $X_{6,t}^{11} = X_{6,t-1}^{11} + 1$

Table A7 Human scientist modeling (HS)

Attribute	Notation	Description	Value
Name	HS		
id	7		
Coupling inputs	$X_{3,t}^{0}$	Ambient temperature	
	$X_{3,t}^{1}$	Ambient pressure	
	$X_{4,t}^{1}$	Science Task requirement	{None, Science}
Control inputs	-	-	
External disturbances	-	-	
States	$X_{7,t}^{0}$	HS default status	
	$X_{7,t}^{1}$	HS availability	
	$X_{7,t}^{2}$	HS status	
	$X_{7,t}^{3}$	HS oxygen consumption	
	$X_{7,t}^{4}$	HS water consumption	
	$X_{7,t}^{5}$	HS food consumption	
	$X_{7,t}^{6}$	HS science outcome	
	$X_{7,t}^{7}$	Hazard indicator	{True, False}
Parameters	θ_7^0	HS default status parameters	
	θ_7^1	HS oxygen parameters: [skewness, mean, standard deviation]	
	θ_7^2	HS water parameters: [mean, standard deviation]	
	θ_7^3	HS food parameters: [mean, standard deviation]	
Coupled parameters	-	-	
State transition functions		$X_{7,t}^{0}$: Table A7-1	
		$X_{7,t}^{1}$: Table A7-2	
		$X_{7,t}^{2}$: Table A7-3	
		$X_{7,t}^{3}$: Table A7-4	
		$X_{7,t}^{4}$: Table A7-5	
		$X_{7,t}^{5}$: Table A7-6	
		$X_{7,t}^{6}$: Table A7-7	
		$X_{7,t}^{7}$: Table A7-8	

Table A7-1 State transition function of HS default status ($X_{7,t}^{0}$)

Output	$X_{7,t}^{0}$

Pseudo code	$X_{7,t}^{0} = f(t)$:
	if $\theta_7^0[0] < t\%24 \leq \theta_7^0[1]$:
	  $X_{7,t}^{0}$ = "Sleeping"
	else if $\theta_7^0[2] < t\%24 \leq \theta_7^0[3]$ or $\theta_7^0[4] < t\%24 \leq \theta_7^0[5]$ or $\theta_7^0[6] < t\%24 \leq \theta_7^0[7]$:
	  $X_{7,t}^{0}$ = "Eating"
	else if $\theta_7^0[8] < t\%24 \leq \theta_7^0[9]$:
	  $X_{7,t}^{0}$ = "Exercising"
	else:
	  $X_{7,t}^{0}$ = "Idle"

Table A7-2 State transition function of HS status ($X_{7,t}^{1}$)

Output	$X_{7,t}^{1}$

Pseudo code	$X_{7,t}^{1} = f(t)$:
	if $X_{7,t}^{0}$ == "Idle":
	  $X_{7,t}^{1}$ = True
	else:
	  $X_{7,t}^{1}$ = False

Table A7-3 State transition function of HS status ($X_{7,t}^{2}$)

Output	$X_{7,t}^{2}$

Pseudo code	$X_{7,t}^{2} = f(t)$:
	if $X_{4,t}^{0}$!= "None":
	  $X_{7,t}^{2}$ = "Science"
	else:
	  $X_{7,t}^{2} = X_{7,t}^{0}$

Table A7-4 State transition function of HS oxygen consumption ($X_{7,t}^{3}$)

Output	$X_{7,t}^{3}$

Pseudo code	$X_{7,t}^{3} = f(t)$:
	if $X_{7,t}^{3}$ == "Exercising":
	  sample ~ D($\alpha = 1.2 * \theta_7^1[0], \xi = \theta_7^1[1], \omega = \theta_7^1[2]$)
	else:
	  sample ~ D($\alpha = \theta_7^1[0], \xi = \theta_7^1[1], \omega = \theta_7^1[2]$)
	  $X_{7,t}^{3} = X_{7,t-1}^{3}$ + sample

Table A7-5 State transition function of HS water consumption ($X_{7,t}^{4}$)

Output	$X_{7,t}^{4}$

Pseudo code	$X_{7,t}^{4} = f(t)$:
	if $X_{7,t}^{4}$ == "Exercising":
	  sample ~ D($\alpha = 2, \xi = \theta_7^2[0], \omega = \theta_7^2[1]$)
	else:
	  sample ~ N($\mu = \theta_7^2[0], \delta = \theta_7^2[1]$)
	  $X_{7,t}^{4} = X_{7,t-1}^{4}$ + sample

Table A7-6 State transition function of HS food consumption ($X_{7,t}^{5}$)

Output	$X_{7,t}^{5}$

Pseudo code	$X_{7,t}^{5} = f(t)$:
	if $X_{7,t}^{5}$ == "Eating":
	  sample ~ N($\mu = \theta_7^3[0], \delta = \theta_7^3[1]$)
	  $X_{7,t}^{5} = X_{7,t-1}^{5}$ + sample

Table A7-7 State transition function of HS science outcome ($X_{7,t}^{6}$)

Output	$X_{7,t}^{6}$
Pseudo code	$X_{7,t}^{6} = f(t)$: if $X_{7,t}^{2}$ == "Science": $X_{7,t}^{6} = X_{7,t-1}^{5} + 1$

Table A7-8 State transition function of hazards indicator ($X_{7,t}^{7}$)

Output	$X_{7,t}^{7}$

Pseudo code	$X_{7,t}^{7} = f(t)$:
	if $X_{3,t}^{0} > 18$ or $X_{3,t}^{0} > 27$ or $X_{3,t}^{1} < 48$ or $X_{3,t}^{1} > 102.7$:
	$X_{7,t}^{7} =$ True
	else:
	$X_{7,t}^{7} =$ False

Table A8 Additional M-ESM cost relating to the change of task speed and task success probability

Input and Output	task speed coefficient, as s task success probability coefficient, as r M-ESM terms relevant to HA, as C_{HA} M-ESM terms relevant to RA, as C_{RA} Modified M-ESM terms relevant to HA, as C'_{HA} Modified M-ESM terms relevant to RA, as C'_{RA}

Pseudo code	f(x,c):
	if $x == 1$:
	return 1
	else if $x > 1$:
	return $1 + c * (x - 1)$
	else:
	return $1 - c * (1 - x)$
	$C'_{HA} = C_{HA} * f(max\ (s,r), 0.5)$
	$C'_{RA} = C_{RA} * f(max\ (s,r), 200)$

Funding Sources

This work was supported by a Space Technology Research Institutes Grant (number 80NSSC19K1076) from NASA's Space Technology Research Grants Program.

References

[1] Uri, J., "Remembering Yuri Gagarin 50 Years Later," Mar 27 2018. Retrieved 1 December 2024. https://www.nasa.gov/history/remembering-yuri-gagarin-50-years-later/

[2] NASA, "July 20, 1969: One Giant Leap For Mankind," Jul 20 2019. Retrieved 1 December 2024. https://www.nasa.gov/history/july-20-1969-one-giant-leap-for-mankind/

[3] NASA, "Space Shuttle Era Facts," April 2012. https://www3.nasa.gov/centers/kennedy/pdf/566250main_SHUTTLE%20ERA%20FACTS_040412.pdf

[4] Szocik, K., and Braddock, M., "Why Human Enhancement Is Necessary for Successful Human Deep-Space Missions," *The New Bioethics*, Vol. 25, No. 4, 2019, pp. 295–317. Retrieved 4 December 2024. http://dx.doi.org/10.1080/20502877.2019.1667559

[5] Donahue, B. B., and Cupples, M. L., "Comparative Analysis of Current NASA Human Mars Mission Architectures," *Journal of Spacecraft and Rockets*, Vol. 38, No. 5, 2001, pp. 745–751. http://dx.doi.org/10.2514/6.2000-3215

[6] Piantadosi, C. A., "Mankind beyond Earth: The History, Science, and Future of Human Space Exploration," Columbia University Press, 2013. http://dx.doi.org/10.7312/columbia/9780231162432.001.0001

[7] Space Station Research Integration Office, "Why Do Research On The International Space Station?," Jul 24 2022. Retrieved 1 December 2024. https://www.nasa.gov/missions/station/iss-research/why-do-research-on-the-international-space-station/

[8] Burns, J. O., Kring, D. A., Hopkins, J. B., Norris, S., Lazio, T. J. W., and Kasper, J., "A Lunar L2-Farside Exploration and Science Mission Concept with the Orion Multi-Purpose Crew Vehicle and a Teleoperated Lander/Rover," *Advances in space research*, Vol. 52, No. 2, 2013, pp. 306–320. http://dx.doi.org/10.1016/j.asr.2012.11.016

[9] Council, N. R., Behavioral, D. of, Sciences, S., Statistics, C. on N., Engineering, D. on, Sciences, P., Board, S. S., Aeronautics, Board, S. E., and Spaceflight, C. on H., "Pathways to Exploration: Rationales and Approaches for a US Program of Human Space Exploration," National Academies Press, 2014. https://nap.nationalacademies.org/catalog/18801/pathways-to-exploration-rationales-and-approaches-for-a-us-program

[10] Dorais, G., Bonasso, R. P., Kortenkamp, D., Pell, B., and Schreckenghost, D., "Adjustable Autonomy for Human-Centered Autonomous Systems on Mars," 1998. https://marspapers.org/paper/MAR98044.pdf

[11] Rader, S. N., and Reagan, M. L., "Human-in-the-Loop Operations over Time Delay: Lessons Learned," 2013. http://dx.doi.org/10.2514/6.2013-3520

[12] Williams, D., Kuipers, A., Mukai, C., and Thirsk, R., "Acclimation during Space Flight: Effects on Human Physiology," *CMAJ. Canadian Medical Association Journal*. 13. Volume 180, 1317–1323. http://dx.doi.org/10.1503/cmaj.090628

[13] Mcphee, J. C., and Charles, J. B., "Human Health and Performance Risks of Space Exploration Missions Evidence," 2009. https://humanresearchroadmap.nasa.gov/Evidence/reports/EvidenceBook.pdf

[14] Kanas, N., and Manzey, D., "Space Psychology and Psychiatry," January 2008. http://dx.doi.org/10.1007/978-1-4020-6770-9

[15] National Academies of Sciences, E. and M., "NASA Space Technology Roadmaps and Priorities Revisited," National Academies Press, Washington, D.C., 2016. http://dx.doi.org/10.17226/23582

[16] Huang, H.-M., Pavek, K., Novak, B., Albus, J., and Messina, E., "A Framework For Autonomy Levels For Unmanned Systems (ALFUS)," 2005. https://doi.org/10.6028/nist.sp.1011-i-2.0

[17] Diftler, M. A., Mehling, J. S., Abdallah, M. E., Radford, N. A., Bridgwater, L. B., Sanders, A. M., Askew, R. S., Linn, D. M., Yamokoski, J. D., and Permenter, F. A., "Robonaut 2-the First Humanoid Robot in Space," 2011. http://dx.doi.org/10.1109/ICRA.2011.5979830

[18] Nesnas, I. A. D., Fesq, L. M., and Volpe, R. A., "Autonomy for Space Robots: Past, Present, and Future," *Current Robotics Reports*, Vol. 2, No. 3, 2021, pp. 251–263. http://dx.doi.org/10.1007/s43154-021-00057-2

[19] Diftler, M. A., and Ambrose, R. O., "Robonaut: A Robotic Astronaut Assistant," Vol. 2001, 2001. https://citeseerx.ist.psu.edu/document?repid=rep1&type=pdf&doi=f4f25b81ac3adb4cb8dad445a0406c824b11c9ff

[20] Landis, G. A., "Robots and Humans: Synergy in Planetary Exploration," Vol. 654, 2003, pp. 853–860. http://dx.doi.org/10.1063/1.1541377

[21] Chitta, S., Jones, E. G., Ciocarlie, M., and Hsiao, K., "Mobile Manipulation in Unstructured Environments: Perception, Planning, and Execution," *IEEE Robotics & Automation Magazine*, Vol. 19, No. 2, 2012, pp. 58–71. http://dx.doi.org/10.1109/MRA.2012.2191995

[22] Kim, W. S., "Developments of New Force Reflecting Control Schemes and an Application to a Teleoperation Training Simulator," 1992. http://dx.doi.org/10.1109/ROBOT.1992.220152

[23] Ryan, M., "Man-Machine Teaming for Future Ground Forces," Center for Strategic and Budgetary Assessments, 2018. https://csbaonline.org/uploads/documents/Human_Machine_Teaming_FinalFormat.pdf

[24] Bernard, D. E., Dorais, G. A., Fry, C., Gamble, E. B., Kanefsky, B., Kurien, J., Millar, W., Muscettola, N., Nayak, P. P., and Pell, B., "Design of the Remote Agent Experiment for Spacecraft Autonomy," Vol. 2, 1998, pp. 259–281. http://dx.doi.org/10.1109/AERO.1998.687914

[25] Volpe, R., "Rover Functional Autonomy Development for the Mars Mobile Science Laboratory," Vol. 2, 2003, pp. 643–652. http://dx.doi.org/10.1109/AERO.2003.1235474

[26] NASA, "Lunar Logistics Drivers and Needs," January 2024. https://www.nasa.gov/wp-content/uploads/2024/01/lunar-logistics-drivers-and-needs.pdf?emrc=6bdbf4

[27] Moon to Mars Architecture, "Https://Www.Nasa.Gov/MoonToMarsArchitecture/," Oct 25 2024. Retrieved 10 December 2024. https://www.nasa.gov/MoonToMarsArchitecture/

[28] Crawford, I. A., Anand, M., Cockell, C. S., Falcke, H., Green, D. A., Jaumann, R., and Wieczorek, M. A., "Back to the Moon: The Scientific Rationale for Resuming Lunar Surface Exploration," *Planetary and Space Science*, Vol. 74, No. 1, 2012, pp. 3–14. http://dx.doi.org/10.1016/j.pss.2012.06.002

[29] Lester, D., and Thronson, H., "Human Space Exploration and Human Spaceflight: Latency and the Cognitive Scale of the Universe," *Space Policy*, Vol. 27, No. 2, 2011, pp. 89–93. http://dx.doi.org/10.1016/j.spacepol.2011.02.002

[30] Malone, T. B., and Permenter, K. E., "Human Factors Issues in Telerobotic Systems for Space Station Freedom Servicing," 1990. https://ntrs.nasa.gov/citations/19900016240

[31] Behjat, A., Liu, X., Forero, O., Ibrahimov, R., Dyke, S., Bilionis, I., Ramirez, J., and Whitaker, D., "A Computational Framework for Making Early Design Decisions in Deep Space Habitats," *Advances in Engineering Software*, Vol. 195, 2024, p. 103690. http://dx.doi.org/10.1016/j.advengsoft.2024.103690

[32] Kanas, N., and Kanas, N., "Psychosocial Issues during an Expedition to Mars," *The new martians: A scientific novel*, 2014, pp. 103–123. http://dx.doi.org/10.1007/978-3-319-00975-9_2

[33] Thangavel, K., Sabatini, R., Gardi, A., Ranasinghe, K., Hilton, S., Servidia, P., and Spiller, D., "Artificial Intelligence for Trusted Autonomous Satellite Operations," *Progress in Aerospace Sciences*, Vol. 144, 2024, p. 100960. http://dx.doi.org/10.1016/j.paerosci.2023.100960

[34] Wilcox, B., and Nguyen, T., "Sojourner on Mars and Lessons Learned for Future Planetary Rovers," SAE Technical Paper, 1998. http://dx.doi.org/10.4271/981695

[35] Huntsberger, T., Aghazarian, H., Baumgartner, E., and Schenker, P. S., "Behavior-Based Control Systems for Planetary Autonomous Robot Outposts," Vol. 7, 2000, pp. 679–686. http://dx.doi.org/10.1109/AERO.2000.879335

[36] Martin, A.-S., "Human-Robotic Cooperative Space Exploration," *Oxford Research Encyclopedia of Planetary Science*, 2022. http://dx.doi.org/10.1093/acrefore/9780190647926.013.219

[37] Singer, S., and Akin, D., "A Survey of Quantitative Team Performance Metrics for Human-Robot Collaboration," 2011. http://dx.doi.org/10.2514/6.2011-5248

[38] Liu, X., Behjat, A., Dyke, S., Whitaker, D., Ramirez, J., and Bilionis, I., "Roles of Human and Robotic Agents toward Operating a Smart Space Habitat," 2023. https://ttu-ir.tdl.org/items/c9e2eb9f-b7ca-474a-b02d-dfb00229da84

[39] Behjat, A., Ibrahimov, R., Lenjani, A., Barket, A., Martinus, K., Maghareh, A., Whitaker, D., Bilionis, I., and Dyke, S., "A Computational Framework for the Evaluation of Resilience in Deep Space Habitat Systems," Vol. 86229, 2022, pp. V03AT03A036. http://dx.doi.org/10.1115/DETC2022-89132

[40] Pritchard, K., Vaccino, L., Liu, X., Whitaker, D., Dyke, S., and Joyal, B., "Lunar SmartHab Mission Operations and Crew Day-In-The-Life," 2023. https://ttu-ir.tdl.org/items/fc009078-c226-4d76-a50f-6ff7e2dc0e00

[41] Dyke, S. J., Marais, K., Bilionis, I., Werfel, J., and Malla, R., "Strategies for the Design and Operation of Resilient Extraterrestrial Habitats," Vol. 11591, 2021, pp. 1159105. http://dx.doi.org/10.1117/12.2585118

[42] Anderson, M. S., Ewert, M. K., and Keener, J. F., "Life Support Baseline Values and Assumptions Document," 2018. https://ntrs.nasa.gov/api/citations/20210024855/downloads/BVAD_2.15.22-final.pdf

[43] Marriott, B. M., "Not Eating Enough: Overcoming Underconsumption of Military Operational Rations," 1995. https://doi.org/10.17226/5002

[44] Sternberg, D. A., Ballard, K., Hardy, J. L., Katz, B., Doraiswamy, P. M., and Scanlon, M., "The Largest Human Cognitive Performance Dataset Reveals Insights into the Effects of Lifestyle Factors and Aging," *Frontiers in human neuroscience*, Vol. 7, 2013, p. 292. http://dx.doi.org/10.3389/fnhum.2013.00292

[45] Kyurkchiev, N., and Markov, S., "Sigmoid Functions: Some Approximation and Modelling Aspects," *LAP LAMBERT Academic Publishing, Saarbrucken*, Vol. 4, 2015. Retrieved 4 December 2024. https://www.biomath.bg/s%20markov%20publications/B2015-Kyurkchiev_Markov_Lambert.pdf

[46] Boston Dynamics, "Spot Specifications," Sep 24 2024. Retrieved 2 December 2024. https://support.bostondynamics.com/s/article/Spot-Specifications-49916

[47] Hoke, A., Brissette, A., Smith, K., Pratt, A., and Maksimovic, D., "Accounting for Lithium-Ion Battery Degradation in Electric Vehicle Charging Optimization," *IEEE Journal of Emerging and Selected Topics in Power Electronics*, Vol. 2, No. 3, 2014, pp. 691–700. http://dx.doi.org/10.1109/JESTPE.2014.2315961

[48] Bousdekis, A., Magoutas, B., Apostolou, D., and Mentzas, G., "A Proactive Decision Making Framework for Condition-Based Maintenance," *Industrial Management & Data Systems*, Vol. 115, No. 7, 2015, pp. 1225–1250. http://dx.doi.org/10.1108/IMDS-03-2015-0071

[49] Department of Energy, "Extend the Operating Life of Your Motor," Nov2012. Retrieved 2 December 2024. https://www.energy.gov/eere/amo/articles/extend-operating-life-your-motor#:~:text=The%20best%20safeguard%20against%20thermal,even%20within%20the%20service%20factor

[50] National Center for Health Statistics, "Body Measurements," Sep 10 2021. Retrieved 2 December 2024. https://www.cdc.gov/nchs/fastats/body-measurements.htm

[51] Jones, H. W., "Oxygen Storage Tanks Are Feasible for Mars Transit," 2017. https://ntrs.nasa.gov/api/citations/20200001084/downloads/20200001084.pdf

[52] Yeoman, D. A., Shkedi, B., and Tobias, B., "International Space Station Water System Architecture and Operational Plan," *SAE International Journal of Aerospace*, Vol. 1, Nos. 2008-01–2007, 2008, pp. 71–77. http://dx.doi.org/10.4271/2008-01-2007

[53] Levri, J., Fisher, J. W., Jones, H. W., Drysdale, A. E., Ewert, M. K., Hanford, A. J., Hogan, J. A., Joshi, J., and Vaccari, D. A., "Advanced Life Support Equivalent System Mass Guidelines Document," 2003. https://ntrs.nasa.gov/api/citations/20040021355/downloads/20040021355.pdf

[54] NASA, "Moon to Mars Objectives," Sep2022. Retrieved 2 December 2024. https://www.nasa.gov/wp-content/uploads/2022/09/m2m-objectives-exec-summary.pdf?emrc=119caf

[55] Smith, M., Craig, D., Herrmann, N., Mahoney, E., Krezel, J., McIntyre, N., and Goodliff, K., "The Artemis Program: An Overview of NASA's Activities to Return Humans to the Moon," 2020. http://dx.doi.org/10.1109/AERO47225.2020.9172323

[56] Lu, X., Wang, P., Niyato, D., Kim, D. I., and Han, Z., "Wireless Charging Technologies: Fundamentals, Standards, and Network Applications," *IEEE communications surveys & tutorials*, Vol. 18, No. 2, 2015, pp. 1413–1452. https://ieeexplore.ieee.org/stamp/stamp.jsp?arnumber=7327131